LOAN COPY

A PRELIMINARY ANALYSIS OF THE M140 RECOIL MECHANISM

by

Arthur D. Newsham, Enzo O. Macagno, and Tin-Kan Hung

Conducted as Part of the
Research Study of the Hydrodynamics of
Recoil Systems
Sponsored by
U.S. Army Rock Island Arsenal
Contract No. DA-11-070-508-ORD-988

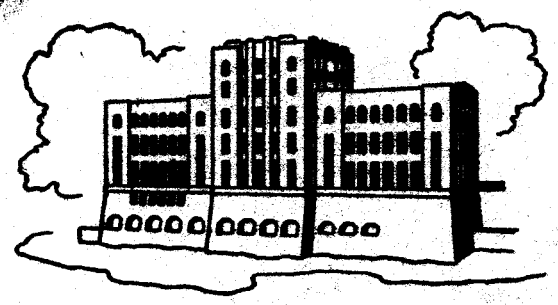

IIHR Report No. 100
Iowa Institute of Hydraulic Research
The University of Iowa
Iowa City, Iowa

December 1966

Distribution. Each transmittal of this document outside the Department of Defense must have prior approval of the R. & E. Division, Rock Island Arsenal.

The findings of this report are not to be construed as an official Department of the Army position, unless so designated by other authorized documents.

Disposition Instruction. Destroy this report when it is no longer needed. Do not return to the originator.

A PRELIMINARY ANALYSIS OF THE M140 RECOIL MECHANISM

by

Arthur D. Newsham, Enzo O. Macagno, and Tin-Kan Hung

Conducted as Part of the
Research Study of the Hydrodynamics of
Recoil Systems
Sponsored by
U.S. Army Rock Island Arsenal
Contract No. DA-11-070-508-ORD-988

Each transmittal of this document outside
the Department of Defense must have prior
approval of the R. & E. Division,
Rock Island Arsenal.

IIHR Report No. 100
Iowa Institute of Hydraulic Research
The University of Iowa
Iowa City, Iowa

December 1966

TABLE OF CONTENTS

INTRODUCTION

Late in 1965, a report entitled "Analysis of the XM37 Recoil Mechanism" [1] was presented in connection with a study being conducted at the Iowa Institute of Hydraulic Research for the Rock Island Arsenal. In December, 1965, a subsequent report was completed, outlining the effect of the steady discharge coefficient and guide friction on the analysis of the XM37 Recoil Mechanism [2]. In the present report the M140 Recoil Mechanism, including the coil spring, is analyzed in a manner similar to that followed for the XM37 Recoil Mechanism.

In addition to obtaining information on the geometry of the M140 Recoil Mechanism, a pumping test similar to that performed on the XM37 has been completed to evaluate the effective bulk modulus. Since no meaningful analysis of the recoil mechanism can be performed without data obtained by subjecting the mechanism to firing conditions, tests were conducted on one of the powder "gymnasticators" at the Rock Island Arsenal. The pertinent results for a number of rounds have been reduced and analyzed.

In spite of differences in geometry and kinematics, the M140 Recoil Mechanism is quite similar to the XM37 Recoil Mechanism in that the mass of fluid is small relative to the mass of the recoiling parts and the maximum pressure changes occurring during the recoil cycle are of similar magnitude for both mechanisms. The total time required for recoil on the M140 is approximately 50 percent of that on the XM37, while the maximum recoil distance is only 25 percent of that for the XM37. Consequently, it may be expected that the accelerations observed for the M140 will not be significantly different from those found for the XM37. In the light of these similarities, it becomes apparent that the analysis of the fluid system of M140 can be analogous to that for the XM37. There is, however, a major difference between the analytical procedure used for the M140 and

---

[1] Newsham, A.D., Macagno, E.O., and Hubbard, P.G., "Analysis of the XM37 Recoil Mechanism," I.I.H.R. Progress Report, 1965.

[2] Newsham, A.D., Macagno, E.O., and Hung, C-Y., "Sliding Friction and Steady-Discharge Coefficient Effects on the Analysis of the XM37 Recoil Mechanism," I.I.H.R. Progress Report, December 1965.

that used for the XM37. This difference stems from the fact that the present analysis can be used directly in the design phase rather than only providing a check on an already completed design. More specifically, the present procedure defines the cross-sectional area of the control-section for a predefined pressure curve rather than predicting the pressure curve for a given control-section cross-sectional area. This line of attack was illustrated in a progress report of 1961 for a simplified model of the recoil mechanism for which the rate-of-flow curve was determined to satisfy a prescribed pressure curve [3]. In addition to being more useful for design, the computational method presented here exhibits considerably more numerical stability than that used heretofore.

---

[3] Macagno, E.O. and Macagno, M., "Pressure-Wave Analysis for Variable Length of Fluid Column," Ninth IAHR, Dubrovnic, 1961.

ANALYSIS

The M140 Recoil Mechanism, the geometry of which is much simpler than that of the XM37 Recoil Mechanism studied previously [1], could probably be analyzed using the complete one-dimensional compressible-flow equations for the region upstream from the control section [3, 4]. However, the analysis of a simplified system, presented in Appendix A of "Analysis of the XM37 Recoil Mechanism" [1], indicates that the M140 fluid system can be studied using the simplified compressible-flow equations in which the momentum of the fluid column is neglected and the pressure waves do not appear [5]. A simplified set of equations can be used to analyze the M140 Recoil Mechanism because the fluid column is relatively short making the time required for a pressure wave to traverse the fluid region upstream from the control section short compared to the duration of the applied force.

One troublesome feature of the M140 - which should be avoided in future designs - is the complicated control section which will allow the control point to shift during recoil and for a period will produce a dual control, with a significant intermediate pressure. In addition, a new element, the coil spring, which in combination with the fluid system acts to retard the motion, must be investigated carefully to determine if the complete dynamic equations of a coil spring need be utilized or if the usual linear relationship between displacement and force can be assumed without causing significant errors in the analysis. For this initial study, the simplified linear relationship for the spring will be used.

Initial Simplifications. A sketch of the M140 Recoil Mechanism is shown in Fig. 1. To facilitate the analysis, several reasonable simplifying assumptions were made. The simplified system, shown in Fig. 2, was obtained by reducing the control section to three orifices at the primary control points and assuming that there is no interaction between

---

[4] Macagno, E.O. and Hubbard, P., "Research Study of the Hydrodynamics of Recoil Mechanisms," I.I.H.R. Final Report for the Rock Island Arsenal, July 1963.

[5] Macagno, E.O. and Ho, H.W., "Approximate Analysis of a Hydraulic Recoiling Mechanism," I.I.H.R. Progress Report, 1962.

the fluid and the spring.

Due to the motion causing a portion of the recoiling parts to leave the region, it may be seen in Fig. 2 that the total volume occupied by the fluid increases during recoil. Since the initial oil pressure throughout the entire system is atmospheric and the upstream oil pressure, P_1, is well above atmospheric during recoil, the downstream pressure, P_3, must be below atmospheric if the entire system is sealed from the surroundings. Obviously, the oil in the downstream region will vaporize, thereby guaranteeing that no pressure below the vapor pressure of the oil will exist there. On the other hand, if the seal breaks down permitting air to enter the downstream region, the pressure downstream from the control may be as high as atmospheric. The effect of these two possibilities will be investigated later in this study.

Equations Governing the System. The motion of the recoiling parts of the mechanism shown in Fig. 2 can be determined by writing the momentum equation, in the direction, of motion between sections A and C indicated in Figs. 3 and 4. This equation can be written for a coordinate system fixed to the ground, or for a system attached to the recoiling parts. The latter was employed for convenience leaving the expression for the local acceleration in an unspecified form. For a recoil distance, $x(t)$, less than 2.75 inches, the control sections 2 and 3 are effective, as well as the control section 1, and as a result Fig. 3A is applicable. When $x(t) > 2.75$ inches (Fig. 4A) no flow constriction exists at control section 3 and, as a result, control section 2 is also no longer effective. Relating the sum of the forces in the x-direction to the resulting change in momentum gives

$$- \int_{\forall_f} \rho \frac{\partial V}{\partial t} d\forall_f + \Sigma F = \int_c \rho V^2 dS - \int_A \rho V^2 dS \qquad (1)$$

In this equation, ρ is the mass density of the hydraulic fluid, V is the velocity at a prescribed point within the fluid region contained between the two sections A and C, $\forall_f$ is the volume of fluid contained between the two same sections, and ΣF is the summation of the external

forces acting in the x-direction upon the fluid region under consideration. The term

$$\int_{\forall_f} \rho \frac{\partial V}{\partial t} d\forall_f \tag{2}$$

is included to account for the force introduced by the mass acceleration of the fluid.

Due to the volume of fluid contained between sections A and C being small, compressibility effects may be neglected because they will be small relative to the discharge into or out of the control volume being considered. If Q_1 is defined as the discharge through control section 1, incompressible flow gives

$$Q_A = Q_C = Q_1 \qquad \text{and} \qquad \rho_A = \rho_C = \rho \tag{3}$$

when conservation of mass is considered.

From Fig. 3A it may be seen that ΣF will be:

$$\Sigma F = P_1 A_1 - P_3 A_3 - F_r - F_c \tag{4}$$

in which F_r is the total force exerted by the recoiling parts on the fluid, F_c is the force exerted on the fluid by the edge of the interior side of the cylinder at control 3, and P_1 and P_3 are the fluid pressures at the respective sections A and C. A_1 and A are the cross-sectional areas of sections A and C, respectively. Over the section A the velocity distribution may be assumed uniform. Therefore it may be seen that

$$V_A = \dot{x}(t) \tag{5}$$

in which $\dot{x}(t)$ is the instantaneous velocity of the recoiling parts. Due to the proximity of section B to the control sections 2 and 3, the velocity distribution across section B cannot be assumed uniform. Instead, a velocity distribution of the form given in Fig. 3C will be assumed.

Both jets will have the same velocity because the same pressure drop occurs across control sections 2 and 3. This gives

$$\int_C \rho V^2 dS = \rho \, [Q_2 V_{J2} + Q_3 V_{J3}] = \rho (Q_2 + Q_3) V_{J2} \tag{6}$$

where Q_2 and Q_3 are the discharges past the control sections 2 and 3 respectively, and V_{J2} is the velocity of the fluid jets produced downstream from the respective control sections. The assumption of incompressible flow within the control sections demands that

$$Q_1 = Q_2 + Q_3 \tag{7}$$

Introducing Eqs. (4), (5), (6) and (7) into Eq. (1) results in

$$\rho \int_{\forall_f} \frac{\partial V}{\partial t} \, d\forall_f + P_1 A_1 - P_3 A_3 - F_r - F_c = \rho Q_1 [V_{J2} - \dot{x}(t)] \tag{8}$$

A similar application of the momentum between sections B and C in Fig. 3B gives

$$P_2 A_2 - P_3 A_2 - F_c = \rho [Q_3 V_{J2} - Q_1 V_{J1}] \tag{9}$$

where P_2 is the pressure in the region between control section 1 and control sections 2 and 3, A_2 is the area of section B indicated in Fig. 3B, and V_{J1} is the velocity of the jet issuing from control section 1.

Applying the equation for accelerated motion to the recoiling parts gives

$$F - S_m - F_g - F_r = \frac{W}{g} \ddot{x}(t) \tag{10}$$

in which F is the force applied to the recoiling parts by the breech, S_m is the force exerted by the coil spring, F_g is the friction force due to the recoiling parts sliding in the guides, W is the weight of the recoiling parts, g is the acceleration due to gravity, and $\ddot{x}(t)$ is the

acceleration of the recoiling parts.

Combining Eqs. (9) and (10) with Eq. (8) to eliminate F_r and F_c, one has

$$\rho\int_{\forall_f} \frac{\partial V}{\partial t}\, d\forall_f + P_1A_1 - P_3A_3 + \frac{W}{g}\ddot{x}(t) + S_m + F_g - F + P_3A_2$$

$$- P_2A_2 + \rho[Q_3V_{J2} - Q_1V_{J1}] = \rho Q_1[V_{J2} - \dot{x}(t)] \qquad (11)$$

After rearranging terms Eq. (11) simplifies to

$$\frac{W}{g}\ddot{x}(t) + \rho\int_{\forall_f} \frac{\partial V}{\partial t}\, d\forall_f = F - P_1A_1 + P_2A_2 + P_3(A_3 - A_2) - S_m$$

$$- F_g + \rho[Q_1(V_{J1} - \dot{x}(t)) + Q_2V_{J2}] \qquad (12)$$

Since the fluid mass between sections A and C will be much smaller than the mass of the recoiling parts and the mean acceleration of the fluid will be of the same order of magnitude as the acceleration of the recoiling parts, the mass acceleration of the fluid can be neglected, and one obtains

$$\frac{W}{g}\ddot{x}(t) = F - P_1A_1 + P_2A_2 + P_3(A_3 - A_2) - S_m - F_g$$

$$+ \rho[Q_1(V_{J1} - \dot{x}(t)) + Q_2V_{J2}] \qquad (13)$$

This equation applies for $x(t) \leq 2.75$ inches.

When $x(t)$ is greater than 2.75 inches, Fig. 4A is applicable. Again, applying the momentum equation between sections A and C, but considering the velocity distribution at the downstream section to be of the form given in Fig. 4B, one can show that

$$\rho\int_{\forall_f} \frac{\partial V}{\partial t}\, d\forall_f + P_1A_1 - P_3A_3 - F_r = \rho Q_1[V_{J1} - \dot{x}(t)] \qquad (14)$$

Then by applying Eq. (10) and neglecting the mass acceleration of the fluid for reasons already discussed the equation defining the motion of the

recoiling parts is

$$\frac{W}{g}\ddot{x}(t) = F - S_m - F_g - P_1A_1 + P_3A_3 + \rho Q_1[V_{J1} - \dot{x}(t)] \qquad (15)$$

This equation applies for $x(t) > 2.75$ inches.

The magnitude of the applied force $F(t)$ provided by the breech, and the upstream pressure, $P_1(t)$, were obtained from experiments and will be discussed at length in the following section on "Input and Verification Data". The downstream pressure, $P_3(t)$, will be taken to be either atmospheric or the vapor pressure of the oil and the effect of this variation will be discussed in the results. In Table 1, the areas, A_1, A_2, and A_3, the weight of the recoiling parts, W, are given.

Due to the symmetry of the mechanism, no significant lateral forces should be exerted by the guides. Consequently, the magnitude of the sliding friction, F_g, will be defined as

$$F_g = \mu W \qquad (16)$$

where μ is the coefficient of sliding friction and W is the weight of the recoiling parts. The value of μ to be considered, which is identical to that used in the study of the XM37 Recoil Mechanism [2], is indicated in Table 1.

A number of studies [6, 7, 8] to determine the effect of motion on the forces exerted by a coil spring are available in the literature. Initial indications from a computational analysis under way are that the effect of the mass of the spring on the forces exerted by the spring will

---

[6] Dick, J., "Shock Waves in Helical Springs," The Engineer, May 9, 1957.

[7] Lee, H.E., "Wave Propagation in Helical Compression Springs," Proc. of the Fifth Symposium of Applied Mathematics of the American Mathematical Society, June 1952, McGraw-Hill Book Company, Inc., New York, N. Y., 1954.

[8] Hussman, Albrecht, "Schwingunger in Schraubenförmigen Ventilfedern," Dr.-Ing. Dissertation, Technischen Hochschule, Berlin, 1938.

not be negligible. However, since none of the methods outlined in the literature can be applied directly, the spring will be assumed to be massless for this initial study. In a second phase, the dynamic treatment of the spring, now under development, will be applied. Although this simplification may have a noticeable effect on the results, significant information on the importance of other factors can still be obtained. For a massless linear spring the following equations can be written:

$$S_m(t) = S_f(t) \tag{17}$$

and

$$S_m(t) = kx(t) + S_m(0) \tag{18}$$

in which S_m and S_f are the forces exerted by the moving and fixed ends of the coil spring respectively, k is the spring constant given in Table 1, and x is the distance the moving end of the spring has been displaced from its in-battery position. $S_m(0)$ is the static internal elastic force in the spring when the mechanism is in battery and its value is also given in Table 1. All remaining variables in Eq. (13) or Eq. (15), P_2, Q_2, V_{J1}, and V_{J2}, can be determined by considering mass continuity of the fluid, and the discharge equations governing the various constrictions in the control section.

Consider a fixed volume element $\delta\forall$ of length δS and cross-sectional area A. An element of this area could be considered instead, but it is easily seen that, because of the one-dimensional approach, the element could be expanded to the area A without affecting any of the other variables. The total mass of fluid within the volume $\delta\forall$ will vary with time, so by equating the net mass flux into the element to the rate of change of the fluid mass within the volume element, the equation of continuity is obtained as

$$\frac{\partial(\rho A \delta S)}{\partial t} = - \frac{\partial(\rho Q)}{\partial S} \delta S \tag{19}$$

Expanding the partial derivatives and dividing both sides by $A\delta S$, one can find the following expression:

$$\frac{\partial \rho}{\partial t} + \rho \frac{\partial (Q/A)}{\partial S} + \frac{Q}{A} \frac{\partial \rho}{\partial S} = 0 \tag{20}$$

Liquids used in recoil mechanism, as all liquids, are compressible. It is customary to indicate the compressibility of liquids by means of the bulk modulus of elasticity as defined by

$$\frac{1}{B} = - \frac{1}{\forall} \frac{\partial \forall}{\partial P} \tag{21}$$

From Eq. (21) and $\rho \forall = \text{const}$, the following equation of state follows almost immediately

$$\frac{\partial P}{\partial \rho} = \frac{B}{\rho} \tag{22}$$

It is assumed that during a single recoil operation there is not enough variation in temperature to justify the use of a more complete equation of state. The bulk modulus of elasticity depends also on the pressure prevalent in the liquid, but it will be assumed to be constant in the following calculations. Since the density is only a function of the pressure P, the partial derivatives of ρ with respect to S and t, may be written in the form:

$$\frac{\partial \rho}{\partial S} = \frac{\partial \rho}{\partial P} \frac{\partial P}{\partial S} = \frac{\rho}{B} \frac{\partial P}{\partial S} \tag{23}$$

$$\frac{\partial \rho}{\partial t} = \frac{\partial \rho}{\partial P} \frac{\partial P}{\partial t} = \frac{\rho}{B} \frac{\partial P}{\partial t} \tag{24}$$

From the equation of state and continuity, the following equation can now be obtained

$$\frac{\partial P}{\partial t} + B \frac{\partial (Q/A)}{\partial S} + V \frac{\partial P}{\partial S} = 0 \tag{25}$$

As the effects of pressure waves have been shown to be negligible for similar systems [1] and the complete one-dimensional compressible-flow equation will not be considered, variations in pressure with position will be neglected. Consequently, $\partial P/\partial S = 0$ and Eq. (26) can be simplified to

$$\frac{dP}{dt} = - B \frac{d(Q/A)}{dS} \tag{26}$$

At any time t, this equation can be integrated with respect to s ; as neither P nor B are functions of S, the result is simply given by

$$- \frac{A}{B} \frac{dP}{dt} \int_0^{L-x(t)} dS = \int_{Q_{in}}^{Q_{out}} dQ$$

$$- \frac{\forall}{B} \frac{dP}{dt} = Q_{out} - Q_{in} \tag{27}$$

where Q_{in} and Q_{out} are the volume rate of discharge into and out of the region, respectively, and $\forall$ is the volume defined as

$$\forall = A_0[L - x(t)] \tag{28}$$

Applying Eq. (27) to the region upstream from the control section, one obtains

$$A_0\dot{x}(t) = Q_1(t) + \frac{\forall}{B} \frac{dP_1}{dt} \tag{29}$$

in which A_0 is the cross-sectional area of the annular region upstream from the control section, Q_1 is the discharge through the first constriction in the control section, and L is the in-battery length of the annular region upstream from the control section.

Within the control section the fluid has been considered incompressible. The error introduced by assuming no storage in this region is negligible because the compressibility term is small compared to the

discharge into or out of the region. Since the efflux velocity from control sections 2 and 3 must be identical and Eq. (7) must be satisfied,

$$Q_2 = Q_1 \frac{Q_2}{Q_2 + Q_3}$$

$$Q_2 = Q_1 \frac{CD_2AO_2}{CD_2AO_2 + CD_3AO_3} \tag{30}$$

The standard equation for the orifice discharge $Q(t)$ is

$$Q(t) = CD(t)AO(t)\sqrt{\frac{2\Delta P(t)}{\rho}} \tag{31}$$

in which $CD(t)$ is the discharge coefficient for the instantaneous conditions, $AO(t)$ is the minimum cross-sectional area of the constriction, and $\Delta P(t)$ is the pressure drop across the constriction. When Eq. (31) is substituted into Eqs. (29) and (7) for the various discharges, the equation

$$A_0\dot{x}(t) = CD_1AO_1\sqrt{\frac{2}{\rho}(P_1 - P_2)} + \frac{\Psi}{B}\frac{dP_1}{dt} \tag{32}$$

and the expression

$$CD_1AO_1\sqrt{\frac{2}{\rho}(P_1 - P_2)} = [CD_2AO_2 + CD_3AO_3]\sqrt{\frac{2}{\rho}(P_2 - P_3)} \tag{33}$$

are obtained. If both sides of Eq. (33) are squared it can be rearranged to give

$$P_2 = P_1 \left\{ \frac{1 + \left(\frac{CD_2AO_2 + CD_3AO_3}{CD_1AO_1} \right)^2 \frac{P_3}{P_1}}{1 + \left(\frac{CD_2AO_2 + CD_3AO_3}{CD_1AO_1} \right)^2} \right\} \tag{34}$$

When $x(t)$ becomes greater than 2.75 inches the constrictions offered by control sections 2 and 3 no longer exist so that

$$\frac{CD_2AO_2 + CD_3AO_3}{CD_1AO_1} \rightarrow \infty$$

and consequently Eq. (34) reduces to

$$P_2 = P_3 \tag{35}$$

Therefore Eq. (34) is applicable when $x(t) \leq 2.75$ inches and Eq. (35) is applicable when $x(t) > 2.75$ inches. Also, Eq. (32) can be written in the form

$$AO_1 = \frac{A_0[\dot{x}(t) - \frac{L - x(t)}{B}\frac{dP_1}{dt}]}{CD_1\sqrt{\frac{2}{\rho}[P_1 - P_2]}} \tag{36}$$

by introducing Eq. (28) and rearranging terms.

The velocity of the fluid issuing from each of the control sections can be computed quite simply if it is assumed that there is no energy loss between a point a short distance upstream from the control and a point in the jet immediately below the control. Pressure variations due to the acceleration of the fluid will be neglected as they will be small compared to the total pressure drop across a control. The Bernoulli equation in terms of the velocity and pressure at two points A and B may be written as:

$$P_A + \rho\frac{V_A^2}{2} = P_B + \rho\frac{V_B^2}{2} \tag{37}$$

Applying Eq. (37) across control section 1 and then across control section 2, one has

$$P_1 + \rho\frac{V_1^2}{2} = P_2 + \rho\frac{V_{J1}^2}{2} \tag{38}$$

and

$$P_2 + \rho \frac{V_2^2}{2} = P_3 + \rho \frac{V_{J2}^2}{2} \tag{39}$$

herein V_1 and V_2 are respectively the approach velocities upstream from control sections 1 and 2. Since both V_1 and V_2 are small compared to the corresponding jet velocity, their squared values appearing in Eqs. (38) and (39) will be neglected, thus yielding the following equations:

$$V_{J1} = \left[\frac{2}{\rho} P_1 - P_2)\right]^{1/2} \tag{40}$$

and

$$V_{J2} = \left[\frac{2}{\rho}(P_2 - P_3)\right]^{1/2} \tag{41}$$

Utilizing Eqs. (16), (18), (28), (29), (30), (35), (40) and (41), Eqs. (13) and (15) can be rewritten in the form:

$$\frac{W}{g} \ddot{x}(t) = F - P_1A_1 + P_2A_2 + P_3(A_3 - A_2) - kx(t) - S_m(0) - \mu W$$

$$+ \rho A_0 \left\{\dot{x}(t) - \frac{L - x(t)}{B} \frac{dP_1}{dt}\right\} \left\{\left[\frac{2}{\rho}(P_1 - P_2)\right]^{1/2} - \dot{x}(t)\right.$$

$$\left. + \left\{\frac{CD_2AO_2}{CD_2AO_2 + CD_3AO_3}\right\}\left[\frac{2}{\rho}(P_2 - P_3)\right]^{1/2}\right\} \tag{42}$$

which is valid for $x(t) \leq 2.75$ inches; and

$$\frac{W}{g} \ddot{x}(t) = F - P_1A_1 + P_3A_3 - kx(t) - S_m(0) - \mu W$$

$$+ \rho A_0 \left\{\dot{x}(t) - \frac{L - x(t)}{B} \frac{dP_1}{dt}\right\}\left\{\left[\frac{2}{\rho}(P_1 - P_3)\right]^{1/2} - \dot{x}(t)\right\} \tag{43}$$

which applies for $x(t) > 2.75$ inches.

For design purposes, the control-section geometry, or at least some part of it, is generally regarded as an unknown. In the case of the M140 Recoil Mechanism, it appears that the most significant variable in the control section is the area of the first constriction, AO_1. If CD_1, CD_2, CD_3, AO_2, and AO_3 are known, then Eq. (36) in conjunction with Eq. (42) and (34) or Eq. (43), depending upon the value of $x(t)$, can be solved by numerical iteration. In this manner, the motion of the mechanism, $x(t)$, $\dot{x}(t)$, and $\ddot{x}(t)$, and the area of the constriction AO_1 can be determined. All other variables defined by the various equations can then be determined by direct computation.

INPUT AND VERIFICATION DATA

Considerable information is necessary to define the recoiling system and to evaluate the accuracy of the results of its analysis. The data can be divided into two categories. The first, which will be designated input data, includes all information necessary to define the independent variables in the equations. In a study of this type, additional information is necessary to evaluate the accuracy with which the equations predict the dependent variable; this additional information will be referred to as verification data. Whether a specific variable is a dependent variable, rather than an independent variable, depends upon the term that is regarded as the unknown in the equation. For example, for the present problem pressure can be considered the unknown variable and determined in terms of the control-section area. Conversely, the pressure can be considered as a known variable and the same equations solved for the area of the control section. In any case, there will be only one dependent variable for the entire system. Once the equations have been solved for the dependent variable, it is a simple matter to evaluate additional variables that may be of interest. There can be innumerable checks on the system. Some experimental verification data, such as orifice area, can be used for an instantaneous check on the analysis, whereas data on total recoil provide an integrated check on the analysis from the initiation of recoil. Generally, both types of verification data are desirable.

Prototype tests to evaluate the recoil of the M140 Recoil Mechanism were conducted on a powder gymnasticator at the Rock Island Arsenal on April 16, 1965. The powder gymnasticator is very useful as a design tool because it permits much better control of the experiments than field tests even if these are conducted under the most ideal conditions. For the analysis of a recoil system, it is very important that the experimental data be accurate. Of considerably less relative significance is the requirement that the evaluation be conducted under conditions that reproduce exactly what might occur under normal or extreme

no question that the experimental data obtained using the powder gymnasticator are superior to those obtained from field tests, and, in addition, the powder gymnasticator appears to approximate field conditions very closely. Once the results of the analysis agree with the powder-gymnasticator data, it should be a relatively simple step to apply the field conditions to the analysis and predict the actual operation of the recoil mechanism. From the results of tests conducted on April 16, 1965, data on the applied force, upstream pressure, and recoil distance have been obtained for several rounds.

Both the input data and the verification data must be evaluated carefully. In the case of recoil mechanisms in which the experiment is completed in a fraction of a second, many difficulties - which have an effect on the accuracy of the results - are encountered when obtaining the data. For this reason, it is desirable to repeat an experiment a number of times and then compare the data for inconsistencies. Care must be exercised that errors in the experimental data are not interpreted as errors in the mathematical model.

Geometry. Although the geometry has been simplified considerably for the analysis (Fig. 2), the dimensions controlling the dynamics of the mechanism have been retained or have been changed in such a manner that the motion during recoil will not be affected. In Table 1, the annular area, A_0, is the average area of the fluid region upstream from the control section and the length, L, is the length of the upstream fluid region when the mechanism is in battery. The annular areas, A_1, A_2, and A_3, have been defined as the areas over which the respective pressures, P_1, P_2, and P_3, are effective (see Fig. 2). The orifices have been simplified in Fig. 2 but their discharge coefficients CD_2 and CD_3, and their cross-sectional areas, AO_1, AO_2, and AO_3, are defined to reproduce the constrictive effects of the actual control section during the entire recoil phase.

In the analysis, the orifice area, AO_1, is regarded as an unknown and therefore any information provided by a knowledge of the geometry is used to verify results.

Fluid properties. In the M140 Recoil Mechanism, the oil (MIL-O-5606) has a mass density, ρ, of 1.61 lb-sec^2/ft^4. The adiabatic bulk modulus of elasticity of the oil has been determined in a laboratory over the full range of temperatures and pressures at which the system is designed to operate. Rather than laboratory values of the adiabatic bulk modulus, one should use as the measure of the compressibility the relationship between an incremental pressure rise, ΔP, in a closed volume $\forall$ of fluid in the recoil mechanism and the addition of an incremental volume of fluid, $\Delta\forall$, according to the following relationship:

$$\Delta P = B \frac{\Delta\forall}{\forall} \qquad (45)$$

If the container were perfectly rigid, this would give a value of B identical to the bulk modulus of the oil. However, the recoil mechanism is not perfectly rigid, and due to the complicated geometry an accurate calculation of the dilatation of the cylinders with pressure is not possible. The effective bulk modulus of the M140 Recoil Mechanism could only be determined experimentally by a pumping test.

Pumping tests were conducted on an M140 Recoil Mechanism at the Rock Island Arsenal in August, 1965. The results are presented in Table 2 and Fig. 5. For comparison, the adiabatic bulk modulus of the oil, MIL-O-5606, is included in Table 2. It can be seen that the effective bulk modulus indicated by the pumping tests is significantly lower than the adiabatic bulk modulus of the fluid. Although there is considerable scatter in the data, it can be seen that the magnitude of the effective bulk modulus tends to exhibit significant oscillations (broken line in Fig. 5) as the pressure on the fluid is increased. The oscillations are probably due to the system expanding suddenly, then being relatively rigid for a considerable pressure increase and then expanding suddenly again rather than expanding elastically at uniform rate as the pressure is increased.

The kinematic viscosity of the oil, ν, is approximately 4×10^{-4} ft^2/sec at 70°F. The effects of viscosity are neglected in the

present analysis because they are assumed to be rather small. They may, however, have a non-negligible influence and should be investigated for a more refined analysis.

Spring Properties. From Eq. (18) it can be seen that the retarding force provided by the coil spring can be determined in terms of the displacement when the spring constant, k, and the internal elastic force present when the system is in-battery, $S_M(0)$, are known if the mass of the spring is neglected. The values of k and $S_M(0)$ were determined from static tests and are given in Table 1.

Sliding Friction. Since the M140 Recoil Mechanism is axisymmetric and all dynamic forces are applied symmetrically about its axis, the normal force on the rails will not be affected by the magnitude of the various forces acting at any instant as in the case of the XM37 Recoil Mechanism [1]. Consequently, the normal force on the rails will be assumed to be equal to the weight W of the recoiling parts. The rail friction, F_g, will be the normal force on the rails times a coefficient of sliding friction, μ, (Eq. 16)). Based on tests [9] the value of μ has been estimated to be one-third the static value which, for hard steel, if 0.42. Since the value of μ is dependent upon many effects not included in this study, a number of different values will be used, and their effect upon the results will be discussed. In order to investigate the influence of μ on the displacement, several values of μ ranging from 0 to 0.42 were used.

Applied Force. The applied force is determined by multiplying the muzzle area by the data obtained from a Hat-gage pressure cell placed in the muzzle. Since all prototype tests were conducted using a powder gynmasticator, there is no separate method to determine the total applied impulse as is possible by computing the momentum of the projectile and ejected gases in a field test. Therefore the magnitude of the applied force, as given by the Hat-gage, was used without correction. The location of the Hat-gage and application of the force in the gymnasticator test is at the muzzle rather

---

[9] Gray, D. E., co-ord. ed., American Institute of Physics Handbook, McGraw-Hill, 1957.

than at the breech. A force applied to the muzzle end of the gun tube will require a short period of time to be transmitted as an elastic wave along the gun tube to the breech. The time delay has been defined as τ so that

$$F_a(t) = F_e(t - \tau) \tag{46}$$

where F_a is the force applied to the recoil mechanism and F_e is the experimental value of the applied force given by the Hat-gage. The values of F_e for a number of rounds are presented in Table 3. An estimate of the time delay can be determined if the elastic modulus, E, the mass density, σ, and the length, L_g, of the gun tube are known, since:

$$\tau = L_g \sqrt{\frac{\sigma}{E}} \tag{47}$$

Upstream Pressure. The pressure upstream from the control section was monitored during the experiments performed on the powder gymnasticator and the values are tabulated in Table 4. The pressure cell was located at approximately the midpoint of the upstream region when the gun was in battery. The location is not important because the pressure variation throughout the entire region upstream from the control section is of the same order of magnitude as the errors inherent in experimentally determining the pressure.

Displacement. For the experiments on the powder gymnasticator, the distance the mechanism has recoiled from its in-battery position was determined, and is presented in Table 5 with the results for the applied force and the upstream-pressure curve. Since the recoil distance is not required to solve Eqs. (1) or (2), it provides a check on the analysis.

Orifice Area. Similar to the data for displacement, the data for orifice area are not necessary for the solution of Eqs. (1) or (2) and can be used as a verification of the analysis. From the geometry of the mechanism, the orifice area can be expressed as:

$$AO_1(t) = 14.4\ \pi[0.176 - 0.0132\ x(t)] \tag{48}$$

Reliability of Data. A close inspection of Tables 3, 4, and 5 indicates considerable variation in the data from one round to another. It may be seen that the time required to reach the maximum applied force may vary by as much as 20 percent. When compared to the average values of all seven rounds tabulated, the integrated results for each round are consistent within themselves. For example, Round 32 has the highest total applied impulse, the highest integrated value of the upstream pressure, and the greatest maximum-recoil distance. From this, it may be concluded that, although the data are not repeatable for successive rounds, they do appear to be consistent among themselves within each round. It also appears from a comparison of the mean value data tests with each original run that the average values would not be representative because of their lacking internal consistency. It seems then preferable to select the round 26 which possesses the integrated characteristics that agrees best with the results of averaging integrated characteristics of all tests. The round 26 with a certain prescribed value of μ, k, B, etc., as shown in Table 6 is designated hereafter as the standard run.

DISCUSSION OF RESULTS

For the standard run, as defined in the previous chapter, the relative influence of the various forces acting on the recoiling parts has been investigated by means of a momentum-impulse balance, which in addition serves to check the computationally determined net momentum. This quantity was obtained after solving Eqs. (42) and (43) for the acceleration $\ddot{x}(t)$, the velocity $\dot{x}(t)$ and the displacement $x(t)$ with the input data; the computational technique is described in detail in Appendix A. Due to the quite different relative magnitudes of the various impulses, these quantities, which are all referred to the total applied-force impulse, are presented using different scales in Figs. 6 and 7. The forces for which the impulses were calculated are the following: the applied force, the upstream and downstream pressure forces, the dynamic force due to internal fluid jets, the coil-spring force, and the friction force. It should be noticed that some of the terms in Figs. 6 and 7 carry a negative sign. The algebraic sum of the impulses deviates little from the values given by the net momentum curve, the maximum deviation being 0.0005 with reference to the total applied-force impulse. It is obvious from Figs. 6 and 7 that the applied force and the upstream-pressure forces have predominant influence on the recoil dynamics; the other forces have a comparatively small effect.

With the aforementioned input data (see Table 6) the displacement of the recoiling parts and the orifice area at control 1(AO_1) have been computed for comparison with the corresponding measured quantities. In Fig. 8, the calculated and the experimentally determined displacements are given for the standard run. The relative difference is defined as $(x - x_E)/(x_E)_{max}$; herein, x and x_E are respectively the computed and the measured displacement. The error varies between zero and ten percent; with a value of seven percent at the end of the recoil. Figure 9 is based on an assumption made necessary by the fact that more than one control section exists in this mechanism. Because orifices 2 and 3 present sharp edges it has been considered appropriate to use $C_D = 0.611$ for them. The coefficient for orifice 1 is not prescribed; its value C_{D1} can be

calculated if the area AO_1 is known for the computed values of $C_{D1}AO_1$ (Appendix A). On the other hand, if a reasonably good estimate could be made for C_{D1}, the present calculation could be used to determine the orifice area as part of design operations. For the present work a mean value of C_{D1} has been determined by means of

$$C_{D1} = \frac{\Sigma AO_1 C_{D1}}{\Sigma AO_{1E}}$$

using the values of the product $AO_1 C_{D1}$, and the values of AO_{1E}, determined from the known geometry of the M140 mechanism and the computed displacement. With this average C_{D1}, values of AO_1 were calculated and are given in Fig. 9. The relative error $(AO_1 - AO_{1E})/(AO_{1E})_{max}$, shows that the effects of unsteadiness on C_{D1} cannot be neglected for design purposes. This can also be seen from Fig. 10, in which the instantaneous discharge coefficient, obtained from the known value of AO_{1E} and the product $AO_1 C_{D1}$, is given. According to the present analysis, such a determination of C_{D1} is not satisfactory. This is probably due to several reasons; the one-dimensional approach, the neglect of viscous effects in the flow development, and the inaccuracies of the input data being the three that are considered as the most important.

A comparison of deviations in the displacement for different rounds is given in Fig. 11. The corresponding calculations were performed with the same values of the different parameters such as spring constant, downstream pressure, rail-friction coefficient, bulk modulus of elasticity, etc. (see Table 6). This figure shows that there is a general trend in the shape of the error curves, but that quantitatively it is still difficult to obtain information from the experiments without important deviations.

To investigate the influence of variations of the input data a series of calculations was carried out in which one parameter at a time was varied while all the others were kept constant. The function subject to this variation of parameters was the displacement. Figure 12 shows the effect of varying the calibration factor for the applied force; a variation of ±2 percent has quite important effects. It is obvious that the force

must be determined with a high accuracy in the experiments. The data on applied forces were digitalized by direct measurement on the experimentally recorded curves. This introduced a source of error which is believed to have raised the inaccuracy above one percent. In fact, it is necessary, for a refined analysis, to obtain data with errors well below one percent. Because the upstream pressure has a magnitude of the order of that of the applied force, the influence of its calibration factor is also expected to be important. One should bear in mind that the displacement results from a double integration of the applied forces with respect to the time variable. For example, the error curves shown in Fig. 12 do not differ significantly from one another for small values of time but, as the effect of the integration accumulates, they depart more and more. In comparison to other factors, the applied force has a predominant effect on this type of error.

Another effect that must be taken into account is the time delay in the actual application of the force due to the propagation of the applied impulse from the muzzle to the breech. This time has been estimated to be 0.6 millisecond, and is approximately equal to the value of one time interval (δt = 0.794 millisecond) used in these computations. In order to be able to appreciate the effect of variations of this parameter, values of τ equal to δt, $2\delta t$, and $3\delta t$ were selected. The results obtained are given in Fig. 13 and they show that the exact location of the application of the force in time is important.

In a similar manner, the variations of other parameters have been determined and represented graphically. The influence of variations of the values of the downstream pressure, the rail-friction coefficient, the spring constant, the bulk modulus of elasticity of the oil and the internal jet-reactions are shown in the Figs. 14 to 18. It should be noticed that the parameters μ, k, and B, for which very large variations were considered, have less influence compared with the other parameters.

Comparison of the error curves shows immediately that, generally speaking, they present an approximate similarity of shape. They have the common feature that variations of these parameters seem to have little effect on the errors during an initial period of about thirty milliseconds; from there on, the curves tend to diverge more strongly for all the parameters studied.

CONCLUSIONS

The present analysis has shown that the one-dimensional approach with a massless spring constitutes an acceptable first approximation for the study of the M140 recoil mechanism. This analysis has proved to be very useful in determining the relative importance of the different variables involved. According to the computational results, it is clear that the effects of deviations in the values of the bulk modulus of elasticity of the hydraulic oil, the spring constant and the rail-friction coefficient are rather small. On the other hand, the time delay, the downstream pressure and the reaction of internal jets have a much larger influence.

For any future experimental verifications utmost care should be exercised in order to improve the accuracy of the recording of the applied force and upstream pressure. It would also be necessary for a more complete verification to measure the downstream pressure.

Acknowledgements

In addition to providing the experimental data necessary for the analysis, Mr. R. H. Coberly of the Rock Island Arsenal arranged for the pumping tests necessary for the determination of the effective bulk modulus. Of the Institute staff, Mr. D. W. McDougall, Research Associate, supervised the pumping tests and critically revised the manuscript, and Messrs. C. Y. Hung and S. T. Hsu, Research Assistants, reduced the experimental results to digital form and completed the drawings.

Table 1. Standardized Geometry of M140 Recoil Mechanism

a. Recoiling Parts and Coil Spring.

$W = 2650$ lb

$S_m(0) = 3000$ lb

$k = 133$ lb/in.

$\mu = 0.21$

b. Lengths and Annular Areas of Fluid Region.

$A_0 = 50.0$ in.^{2} $\quad A_2 = 24.3$ in.^{2}

$A_1 = 54.0$ in.^{2} $\quad A_3 = 167.5$ in.^{2}

$L = 22.5$ in.

c. Control-Section Geometry.

$AO_{1E} = 7.97 - 0.597\, x(t)$ in.^{2}

$AO_2 = 8.00$ in.^{2}

$AO_3 = 0.212$ in.^{2} for $x(t) < 0.25$ in.

$= 0.212 + 1.0179(x(t) - 0.25)$ in.^{2} for $0.25 \leq x(t) \leq 2.75$ in.

$CD_2 = 0.611$

$CD_3 = 0.611$

d. Gun Tube.

$L_g = 120$ in.

$\sigma = 0.284$ lb/in.^{3}

$E = 30{,}000{,}000$ lb/in.^{2}

Table 2. Fluid-Elastic Properties of M140 Recoil Mechanism

$\rho = 1.61$ slugs/ft^3

$\nu = 4 \times 10^{-4}$ ft^2/sec

Bulk Modulus of Elasticity at 78°F

Pressure psi	Adiabatic Bulk Modulus of the Oil (psi)	Effective Bulk Modulus of the System (psi)
0	234,000	20,000
100	236,000	106,000
200	237,000	123,000
500	242,000	133,000
1000	251,000	135,000
1500	262,000	135,000
2000	272,000	135,000
2500	278,000	135,000

Table 3. Force Applied to M140 Recoil Mechanism From Tests Conducted on April 26, 1966

Time (sec) \ Round No.	Applied Force (lb) 22	24	26	29	30	32	34
0.00000	0	0	0	0	0	0	0
0.00079	9250	9250	5550	5550	5550	7400	7400
0.00159	11100	11100	7400	7400	5550	9250	7400
0.00238	16650	14800	7400	9250	7400	11100	9250
0.00317	20350	20350	9250	11100	7400	14800	9250
0.00397	27750	27750	9250	16650	9250	18500	11100
0.00476	40700	38850	11100	22200	11100	27750	12950
0.00556	55500	55500	12950	31450	14800	42550	14800
0.00635	83250	85100	16650	46250	18500	62900	18500
0.00714	129500	138750	24050	59200	27750	96200	25900
0.00794	185000	185000	33300	83250	37000	148000	33300
0.00873	259000	240500	48100	120250	51800	210900	46250
0.00952	333000	342250	77700	185000	81400	268250	68450
0.01032	379250	379250	114700	277500	120250	327450	101750
0.01111	425500	421800	160950	351500	166500	388500	148000
0.01190	412550	412550	222000	410700	231250	425500	203500
0.01270	379250	370000	296000	414400	292300	407000	268250
0.01349	370000	342250	358900	388500	355200	379250	318200
0.01428	314500	307100	416250	351500	410700	342250	360750
0.01508	286750	281200	425500	323750	429200	318200	416250
0.01587	259000	259000	399600	296000	399600	284900	412550
0.01667	212750	194250	362600	268250	364450	259000	370000
0.01746	120250	120250	333000	249750	333000	222000	338550
0.01825	64750	64750	305250	203500	301550	138750	318200
0.01905	27750	27750	271950	138750	273800	83250	286750
0.01984	12950	12950	240500	92500	247900	31450	259000
0.02063	0	0	166500	46250	185000	16650	218300
0.02143	0	0	88800	18500	101750	3700	138750
0.02222	0	0	37000	9250	46250	1850	74000
0.02301	0	0	18500	3700	24050	0	37000
0.02381	0	0	3700	0	9250	0	14800
0.02460	0	0	0	0	9250	0	14800
Total Impulse (lb-sec)	3522	3464	3564	3527	3636	3611	3624
Percentage Error Relative to Mean Impulse	-1.16	-2.81	-0.01	-1.04	2.01	1.31	1.68

Table 4. Upstream Pressure in M140 Recoil Mechanism From Tests Conducted on April 26, 1966

Time (sec) \ Round No.	Upstream Pressure (lb)						
	22	24	26	29	30	32	34
0.00000	0	0	0	0	0	0	0
0.00079	0	0	0	0	0	0	0
0.00159	0	0	0	0	0	0	0
0.00238	0	0	0	0	0	0	0
0.00317	0	0	0	0	0	0	0
0.00397	0	0	0	0	0	0	0
0.00476	0	0	0	0	0	0	0
0.00556	0	0	0	0	0	0	0
0.00635	0	0	0	0	0	0	0
0.00714	0	0	0	0	0	0	0
0.00794	0	0	0	0	0	0	0
0.00873	2905	0	0	0	0	0	0
0.00952	7263	0	0	0	0	1452	0
0.01032	11620	7263	0	0	0	2905	0
0.01111	17431	14526	0	0	0	7263	0
0.01190	24694	21789	0	5810	0	17431	0
0.01270	31957	29052	0	14526	0	23241	0
0.01349	39220	36315	2905	21789	2905	29052	4357
0.01428	52293	46483	7263	29052	10168	36315	11620
0.01508	65367	62461	17431	36315	17431	46483	17431
0.01587	84250	79893	23241	47935	23241	58104	23241
0.01667	101682	94419	29052	65367	33409	78440	31957
0.01746	123471	116208	37767	79893	40672	94419	36315
0.01825	135091	130734	49388	95871	50841	111850	46483
0.01905	146712	140902	62461	111850	65367	130743	61009
0.01984	156880	152523	84250	130734	87156	142354	79893
0.02063	162691	156880	101682	145260	101682	152523	95871
0.02143	159786	153975	122018	152523	123471	167049	119113
0.02222	153975	149617	135091	162691	136544	165596	133639
0.02301	145260	142354	142354	162691	148165	158333	142354
0.02381	136544	133639	153975	159786	159786	152523	152523
0.02460	124923	122018	162691	148165	167049	139449	164143
0.02540	122018	119113	159786	143807	159786	130734	159786
0.02619	114755	111850	152523	126376	155428	122018	152523
0.02698	110397	108945	145260	119113	142354	116208	145260
0.02778	106039	104587	136544	116208	133639	108945	136544
0.02857	106039	103134	124923	108945	122018	103134	124923
0.02936	101682	98776	120565	104587	116208	98776	119113
0.03016	94419	94419	111850	101682	108945	97324	108945
0.03095	87156	90061	108945	98776	104587	95871	106039
0.03174	79893	81345	104587	95871	101682	92966	98776
0.03254	72630	72630	103134	92966	98776	87156	97324
0.03333	65367	65367	101682	84250	97324	79893	95871

Table 4 Continued

Time (sec) \ Round No.	Upstream Pressure (lb) 22	24	26	29	30	32	34
0.03412	58104	58104	95871	75535	94419	72630	92966
0.03492	52293	52293	90061	65367	87156	65367	87156
0.03571	50841	49388	81345	58104	81345	61009	81345
0.03651	46483	46483	72630	52293	76987	55198	75535
0.03730	46483	45030	66819	49388	69724	53746	68272
0.03809	45030	43578	61009	46483	63914	50841	62461
0.03889	43578	42125	53746	46483	58104	50841	55198
0.03968	43578	42125	52293	46483	53746	50841	52293
0.04047	40672	39220	49388	46483	50841	47935	50841
0.04127	39220	36315	47935	45030	47935	45030	46483
0.04206	36315	36315	49388	43578	49388	43578	46483
0.04285	34862	34862	47935	40672	47935	40672	46483
0.04365	31957	29052	43578	39220	46483	36315	43578
0.04444	29052	27599	40672	36315	43578	34862	42125
0.04524	26146	26146	39220	31957	40672	34862	40672
0.04603	24694	24694	37767	30504	36315	31957	37767
0.04682	24694	23241	36315	30504	33409	30504	34862
0.04762	24694	23241	33409	29052	31957	29052	33409
0.04841	23241	23241	31957	29052	31957	26146	31957
0.04920	23241	21789	27599	27599	30504	26146	29052
0.05000	21789	21789	26146	27599	29052	24694	26146
0.05079	21789	21789	26146	26146	26146	24694	24694
0.05158	20336	20336	26146	24694	24694	23241	23241
0.05238	18883	18883	24694	23241	23241	23241	23241
0.05317	18883	17431	24694	21789	23241	21789	23241
0.05396	17431	15978	23241	21789	21789	20336	21789
0.05476	17431	15978	23241	20336	21789	20336	21789
0.05555	17431	14526	21789	18883	20336	18883	21789
0.05635	14526	14526	20336	14526	20336	18883	20336
0.05714	13073	14526	20336	14526	18883	17431	17431
0.05793	13073	13073	20336	13073	18883	15978	17431
0.05873	13073	13073	18883	13073	17431	15978	17431
0.05952	11620	11620	18883	11620	15978	17431	15978
0.06031	11620	11620	17431	10168	15978	14526	15978
0.06111	10168	10168	17431	10168	14526	14526	15978
0.06190	10168	10168	15968	8715	14526	13073	15978
0.06269	8715	10168	14526	8715	13073	11620	14526
0.06349	8715	8715	13073	7263	13073	11620	14526
0.06428	8715	8715	13073	7263	11620	11620	13073
0.06508	7263	8715	11620	5810	11620	11620	11620
0.06587	7263	7263	11620	5810	10168	10168	11620
0.06666	5810	5810	11620	5810	10168	10168	11620
0.06746	5810	5810	10168	5810	10168	10168	10168
0.06825	5810	5810	10168	5810	8715	8715	10168
0.06904	5810	5810	8715	5810	8715	8715	10168

Table 4 Continued

Time (sec) \ Round No.	Upstream Pressure (lb)						
	22	24	26	29	30	32	34
0.06984	5810	5810	8715	4357	8715	8715	8715
0.07063	4357	4357	8715	4357	7263	8715	8715
0.07142	4357	4357	8715	4357	7263	8715	8715
0.07222	4357	4357	8715	4357	7263	7263	7263
0.07301	4357	4357	8715	4357	7263	7263	7263
0.07380	3257	4357	7263	2905	7263	7263	7263
0.07460	4357	4357	7263	2905	5810	7263	7263
0.07539	4357	4357	7263	2905	5810	5810	7263
0.07619	4357	4357	5810	2905	5810	5810	5810
0.07698	2905	4357	5810	2905	5810	5810	5810
0.07777	2905	2905	5810	1452	4357	4357	5810
0.07857	2905	2905	5810	1452	4357	4357	5810
0.07936	2905	2905	5810	1452	4357	4357	5810
0.08015	2905	2905	4357	1452	4357	4357	5810
0.08095	2905	1452	4357	1452	4357	4357	5810
0.08174	2905	1452	4357	1452	4357	4357	5810
0.08253	2905	0	4357	0	4357	4357	4357
0.08333	2905	0	4357	0	4357	4357	4357
0.08412	2905	0	2905	0	2905	2905	4357
0.08492	2905	0	2905	0	2905	2905	4357
0.08571	2905	0	2905	0	2905	2905	4357
0.08650	2905	0	2905	0	2905	2905	2905
0.08730	1452	0	2905	0	2905	2905	2905
0.08809	1452	0	2905	0	2905	2905	2905
0.08888	1452	0	2905	0	2905	2905	2905
0.08968	1452	0	2905	0	1452	1452	2905
0.09047	1452	0	1452	0	1452	1452	2905
0.09126	1452	0	1452	0	1452	1452	2905
0.09206	1452	0	1452	0	1452	1452	2905
0.09285	1452	0	1452	0	1452	1452	1452
0.09364	1452	0	1452	0	1452	1452	1452
0.09444	1452	0	1452	0	0	1452	1452
0.09523	0	0	1452	0	0	1452	1452
0.09603	0	0	1452	0	0	1452	1452
0.09682	0	0	1452	0	0	1452	1452
0.09761	0	0	1452	0	0	1452	1452
0.09841	0	0	1452	0	0	1452	1452
0.09920	0	0	0	0	0	1452	0
0.09999	0	0	0	0	0	1452	0
0.10079	0	0	0	0	0	1452	0
0.10158	0	0	0	0	0	1452	0
0.10237	0	0	0	0	0	1452	0
0.10317	0	0	0	0	0	1452	0
0.10396	0	0	0	0	0	1452	0

Table 4 Continued

Time (sec) \ Round No.	Upstream Pressure (lb) 22	24	26	29	30	32	34
0.10476	0	0	0	0	0	1452	0
0.10555	0	0	0	0	0	1452	0
0.10634	0	0	0	0	0	1452	0
Total Impulse (lb-sec)	3253	3126	3307	3189	3288	3410	3270
Percentage Error Relative to Mean Impulse	-0.3	-4	1	-2	1	4	0.2

Table 5. Displacement of M140 Recoil Mechanism From Tests Conducted on April 26, 1966

Time (sec) \ Round No.	Displacement (in)						
	22	24	26	29	30	32	34
0.00000	0.000	0.000	0.000	0.000	0.000	0.000	0.000
0.00079	0.000	0.000	0.000	0.000	0.000	0.000	0.000
0.00159	0.000	0.000	0.000	0.000	0.000	0.000	0.000
0.00238	0.000	0.000	0.000	0.000	0.000	0.000	0.000
0.00317	0.000	0.000	0.000	0.000	0.000	0.000	0.000
0.00397	0.000	0.000	0.000	0.000	0.000	0.000	0.000
0.00476	0.000	0.000	0.000	0.000	0.000	0.000	0.000
0.00556	0.027	0.027	0.000	0.000	0.000	0.000	0.000
0.00635	0.054	0.027	0.000	0.000	0.000	0.000	0.000
0.00714	0.081	0.081	0.000	0.000	0.000	0.000	0.000
0.00794	0.108	0.108	0.000	0.000	0.000	0.027	0.000
0.00873	0.162	0.135	0.000	0.000	0.000	0.054	0.000
0.00952	0.216	0.162	0.000	0.054	0.000	0.108	0.000
0.01032	0.324	0.270	0.000	0.135	0.027	0.162	0.000
0.01111	0.405	0.405	0.027	0.162	0.027	0.189	0.000
0.01190	0.567	0.540	0.081	0.270	0.054	0.378	0.081
0.01270	0.729	0.675	0.135	0.378	0.135	0.459	0.135
0.01349	0.891	0.864	0.189	0.513	0.162	0.594	0.216
0.01428	1.107	1.080	0.270	0.675	0.216	0.810	0.270
0.01508	1.350	1.350	0.486	0.864	0.324	0.999	0.405
0.01587	1.620	1.566	0.540	1.080	0.432	1.215	0.540
0.01667	1.971	1.890	0.675	1.350	0.621	1.485	0.729
0.01746	2.214	2.106	0.729	1.566	0.810	1.755	0.945
0.01825	2.484	2.430	1.080	1.836	0.999	2.025	1.161
0.01905	2.808	2.700	1.323	2.106	1.215	2.268	1.350
0.01984	2.997	2.862	1.593	2.430	1.458	2.565	1.620
0.02063	3.294	3.240	1.836	2.700	1.755	2.781	1.890
0.02143	3.510	3.456	2.133	2.970	1.998	2.132	2.160
0.02222	3.861	3.645	2.430	3.240	2.268	3.348	2.484
0.02301	4.185	4.050	2.673	3.456	2.511	3.591	2.781
0.02381	4.455	4.239	2.889	3.672	2.754	3.861	2.970
0.02460	4.698	4.509	3.267	4.050	2.970	4.158	3.240
0.02540	4.941	4.779	3.537	4.266	3.429	4.428	3.564
0.02619	5.184	4.995	3.780	4.536	3.591	4.725	3.861
0.02698	5.454	5.238	4.050	4.779	3.834	4.941	4.104
0.02778	5.670	5.454	4.347	5.049	4.185	5.130	4.320
0.02857	5.886	5.670	4.644	5.319	4.428	5.454	4.617
0.02936	6.075	5.859	4.860	5.562	4.644	5.670	4.914
0.03016	6.210	6.102	5.130	5.751	4.860	5.940	5.130
0.03095	6.534	6.291	5.346	5.940	5.130	6.102	5.346
0.03174	6.696	6.480	5.589	6.156	5.346	6.345	5.616

Table 5 Continued

Time (sec) \ Round No.	Displacement (in) 22	24	26	29	30	32	34
0.03254	6.885	6.669	5.859	6.399	5.535	6.534	5.832
0.03333	7.047	6.831	6.075	6.615	5.805	6.750	6.075
0.03412	7.236	7.047	6.264	6.750	6.048	6.885	6.264
0.03492	7.425	7.155	6.426	6.939	6.210	7.101	6.480
0.03571	7.560	7.290	6.615	7.101	6.399	7.290	6.669
0.03651	7.695	7.452	6.804	7.236	6.615	7.425	6.831
0.03730	7.857	7.641	6.966	7.425	6.750	7.560	7.020
0.03809	8.019	7.749	7.128	7.560	6.966	7.695	7.182
0.03889	8.127	7.911	7.290	7.695	7.101	7.830	7.344
0.03968	8.262	8.046	7.452	7.884	7.236	7.992	7.506
0.04047	8.424	8.208	7.614	7.992	7.425	8.154	7.695
0.04127	8.532	8.316	7.749	8.127	7.560	8.289	7.830
0.04206	8.640	8.451	7.911	8.235	7.722	8.424	7.965
0.04285	8.775	8.559	8.046	8.397	7.884	8.505	8.100
0.04365	8.883	8.694	8.181	8.532	7.911	8.640	8.235
0.04444	8.991	8.802	8.289	8.640	8.154	8.775	8.370
0.04524	9.099	8.910	8.424	8.748	8.262	8.910	8.505
0.04603	9.180	9.018	8.532	8.856	8.424	9.018	8.640
0.04682	9.315	9.099	8.667	8.964	8.532	9.126	8.775
0.04762	9.450	9.180	8.775	9.045	8.640	9.207	8.856
0.04841	9.504	9.315	8.910	9.180	8.775	9.315	8.991
0.04920	9.585	9.450	9.018	9.261	8.910	9.423	9.072
0.05000	9.720	9.504	9.099	9.369	8.991	9.531	9.180
0.05079	9.801	9.585	9.207	9.450	9.099	9.585	9.261
0.05158	9.882	9.666	9.315	9.504	9.180	9.693	9.396
0.05238	9.936	9.774	9.388	9.585	9.288	9.801	9.477
0.05317	10.044	9.855	9.504	9.639	9.396	9.855	9.585
0.05396	10.098	9.936	9.585	9.720	9.477	9.909	9.639
0.05476	10.179	9.990	9.666	9.801	9.585	9.990	9.720
0.05555	10.260	10.071	9.774	9.882	9.639	10.071	9.828
0.05635	10.287	10.125	9.828	9.936	9.720	10.125	9.909
0.05714	10.368	10.179	9.909	10.044	9.828	10.179	9.963
0.05793	10.422	10.206	9.990	10.125	9.909	10.233	10.044
0.05873	10.476	10.287	10.071	10.179	9.963	10.314	10.098
0.05952	10.530	10.368	10.125	10.260	10.044	10.368	10.179
0.06031	10.584	10.449	10.179	10.314	10.098	10.422	10.233
0.06111	10.638	10.503	10.233	10.368	10.152	10.476	10.314
0.06190	10.692	10.557	10.387	10.395	10.233	10.530	10.368
0.06269	10.746	10.611	10.341	10.449	10.260	10.584	10.422
0.06349	10.854	10.665	10.395	10.503	10.341	10.638	10.476
0.06428	10.881	10.719	10.449	10.530	10.395	10.692	10.530
0.06508	10.908	10.746	10.503	10.611	10.449	10.719	10.584
0.06587	10.962	10.827	10.557	10.665	10.530	10.773	10.638

Table 5 Continued

Time (sec) \ Round No.	Displacement (in) 22	24	26	29	30	32	34
0.06666	10.989	10.881	10.611	10.746	10.584	10.827	10.692
0.06746	11.016	10.935	10.665	10.773	10.638	10.881	10.719
0.06825	11.070	10.962	10.719	10.800	10.665	10.908	10.773
0.06904	11.097	10.989	10.773	10.827	10.719	10.962	10.827
0.06984	11.124	11.043	10.800	10.881	10.773	10.989	10.854
0.07063	11.178	11.070	10.854	10.908	10.800	11.016	10.908
0.07142	11.232	11.097	11.881	10.935	10.854	11.043	10.935
0.07222	11.259	11.124	10.908	10.962	10-881	11.070	10.989
0.07301	11.259	11.151	10.935	11.016	10.935	11.124	11.016
0.07380	11.286	11.178	10.989	11.043	10.962	11.151	11.070
0.07460	11.313	11.205	11.043	11.070	11.043	11.178	11.097
0.07539	11.340	11.232	11.070	11.124	11.097	11.205	11.124
0.07619	11.367	11.259	11.097	11.178	11.124	11.232	11.178
0.07698	11.394	11.286	11.124	11.205	11.151	11.259	11.205
0.07777	11.421	11.286	11.151	11.232	11.178	11.286	11.232
0.07857	11.448	11.313	11.178	11.232	11.205	11.313	11.259
0.07936	11.475	11.340	11.205	11.259	11.232	11.340	11.286
0.08015	11.502	11.367	11.232	11.259	11.259	11.367	11.313
0.08095	11.529	11.394	11.259	11.286	11.286	11.394	11.340
0.08174	11.529	11.421	11.286	11.286	11.313	11.421	11.367
0.08253	11.529	11.448	11.313	11.313	11.340	11.421	11.394
0.08333	11.556	11.448	11.340	11.340	11.367	11.448	11.421
0.08412	11.556	11.475	11.340	11.367	11.394	11.475	11.421
0.08492	11.556	11.475	11.367	11.394	11.421	11.502	11.448
0.08571	11.583	11.502	11.367	11.394	11.448	11.529	11.448
0.08650	11.583	11.502	11.394	11.421	11.448	11.529	11.475
0.08730	11.610	11.529	11.394	11.448	11.475	11.556	11.475
0.08809	11.610	11.529	11.421	11.448	11.502	11.556	11.502
0.08888	11.637	11.529	11.421	11.475	11.502	11.556	11.502
0.08968	11.637	11.529	11.448	11.475	11.529	11.583	11.529
0.09047	11.637	11.556	11.448	11.502	11.529	11.583	11.529
0.09126	11.664	11.556	11.475	11.502	11.556	11.610	11.556
0.09206	11.664	11.583	11.475	11.529	11.556	11.610	11.556
0.09285	11.664	11.583	11.502	11.529	11.583	11.637	11.556
0.09364	11.664	11.583	11.502	11.529	11.583	11.664	11.583
0.09444	11.691	11.610	11.502	11.529	11.583	11.691	11.583
0.09523	11.691	11.610	11.529	11.529	11.583	11.691	11.583
0.09603	11.691	11.610	11.529	11.529	11.583	11.691	11.583
0.09682	11.691	11.610	11.529	11.529	11.583	11.691	11.610
0.09761	11.718	11.610	11.529	11.529	11.583	11.691	11.610
0.09841	11.718	11.610	11.556	11.529	11.583	11.691	11.610
0.09920	11.718	11.610	11.556	11.529	11.583	11.691	11.637
0.09999	11.718	11.610	11.556	11.556	11.583	11.691	11.637

Table 5 Continued

Time (sec) \ Round No.	Displacement (in) 22	24	26	29	30	32	34
0.10079	11.718	11.610	11.556	11.556	11.583	11.718	11.637
0.10158	11.718	11.637	11.556	11.556	11.610	11.718	11.664
0.10237	11.718	11.637	11.583	11.556	11.610	11.718	11.664
Percentage Error Relative to Mean Displacement	0.66	-0.03	-0.50	-0.73	-0.27	0.66	0.20

Table 6. Standard-Run Data

Round No. 26

Force calibration factor = 100%

B = 135,000 psi

k = 133 lb/in

μ = 0.21

P_3 = 0

τ = 0

Internal jet-momentum impulse included.

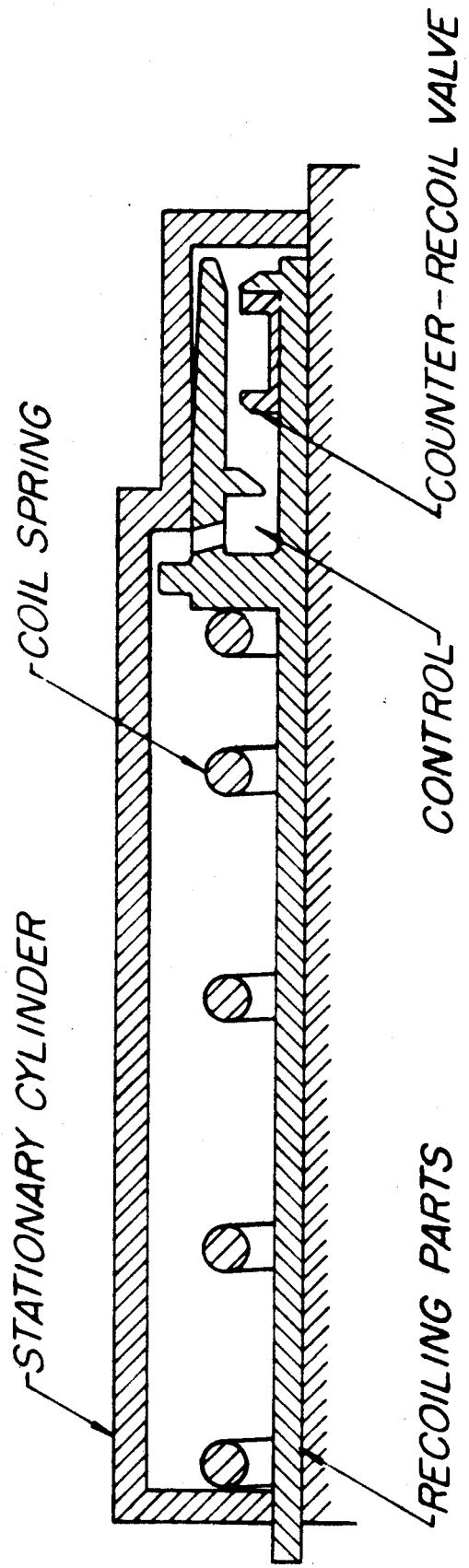

Fig. 1. Sketch of the M140 recoil mechanism

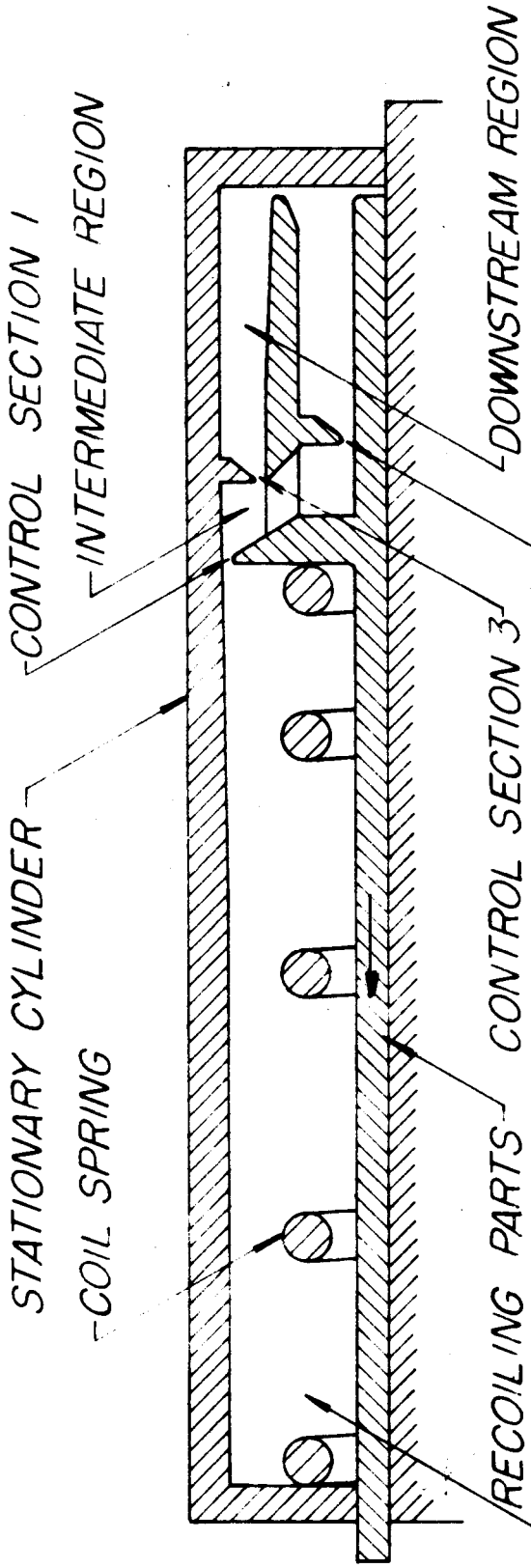

Fig. 2. Definition of control sections, and regions with different pressures for a simplified mechanism

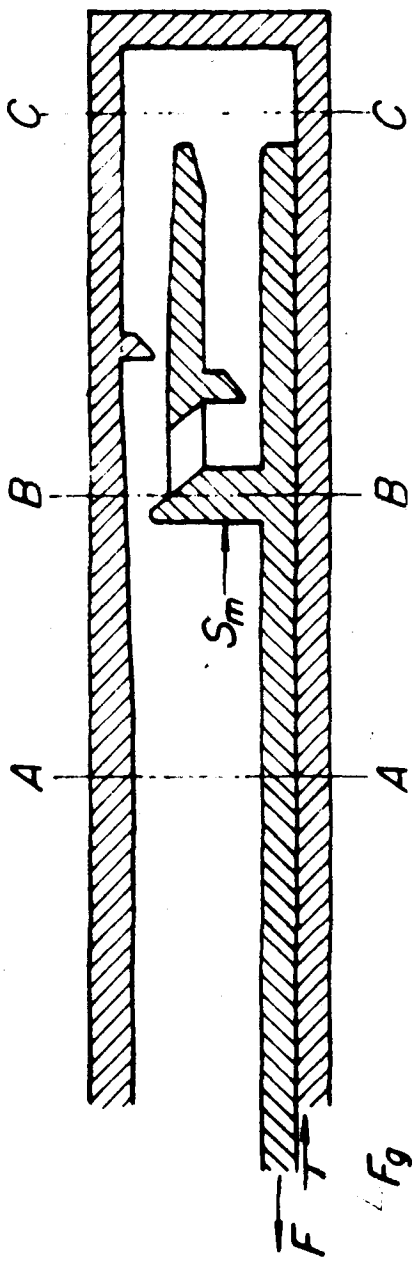

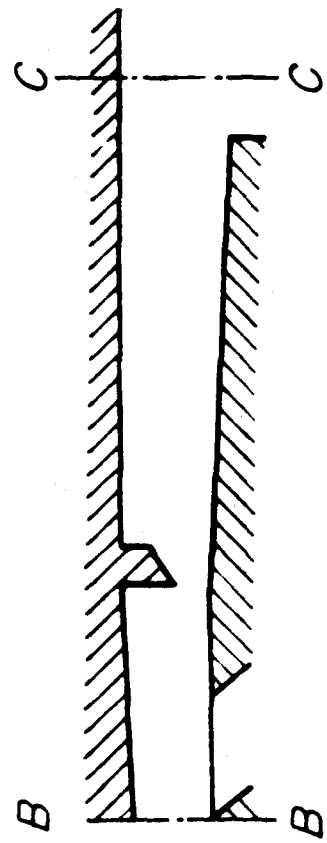

Fig. 3A and 3B. Cross sections and forces used in the calculations

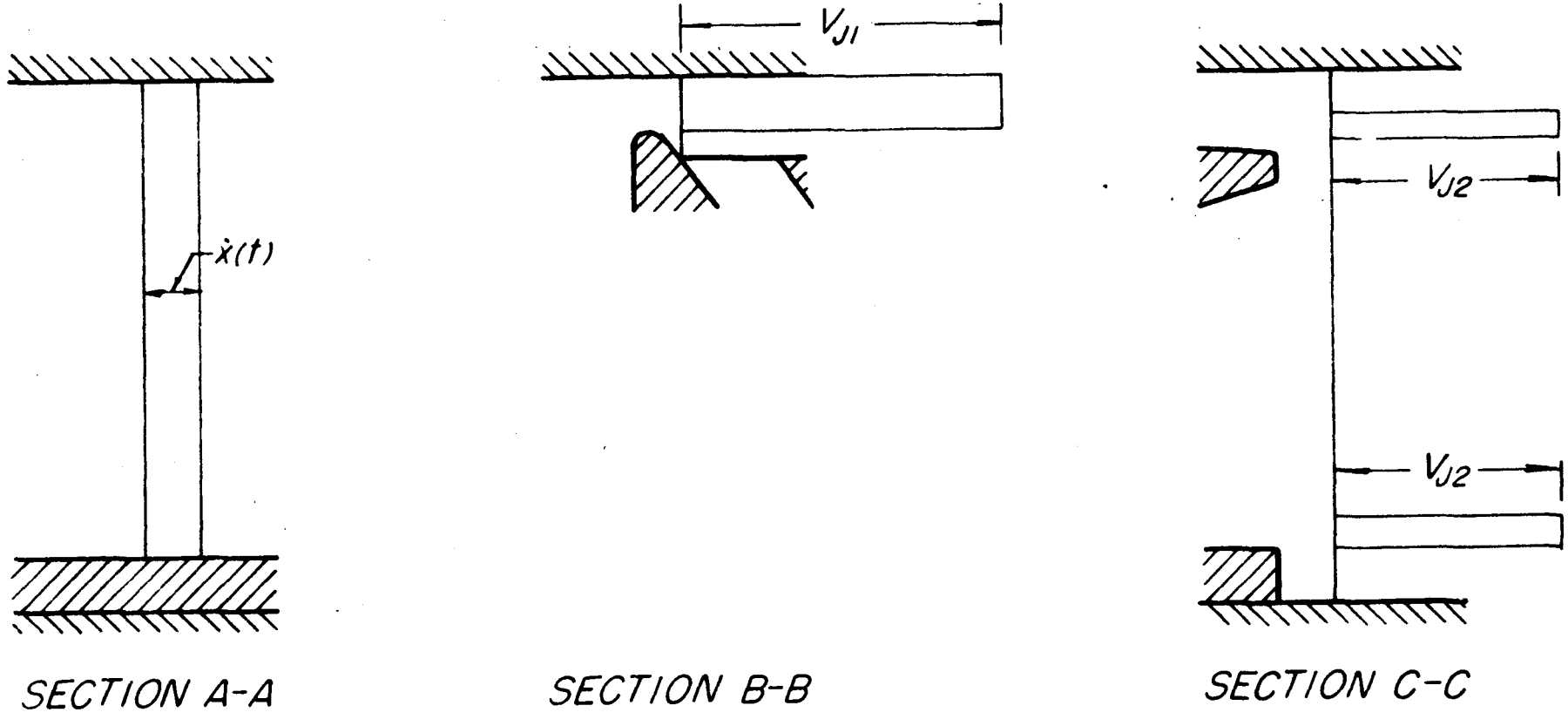

Fig. 3C. Velocities assumed at different sections for the momentum analysis

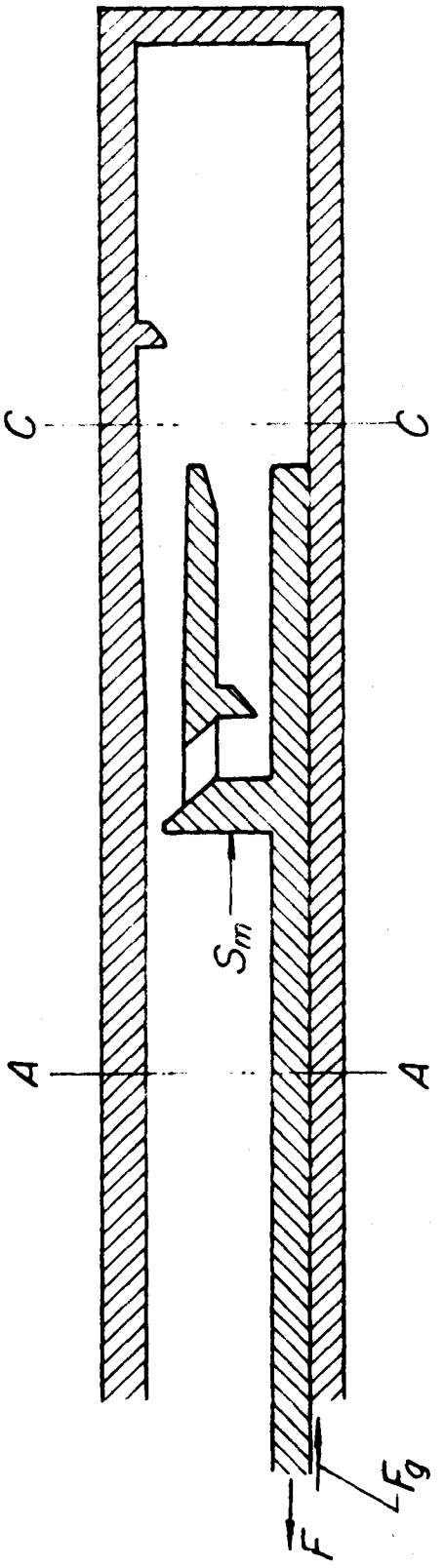

Fig. 4A. Geometry assumed for the second phase in the analysis,
(x(t) > 2.75 inches)

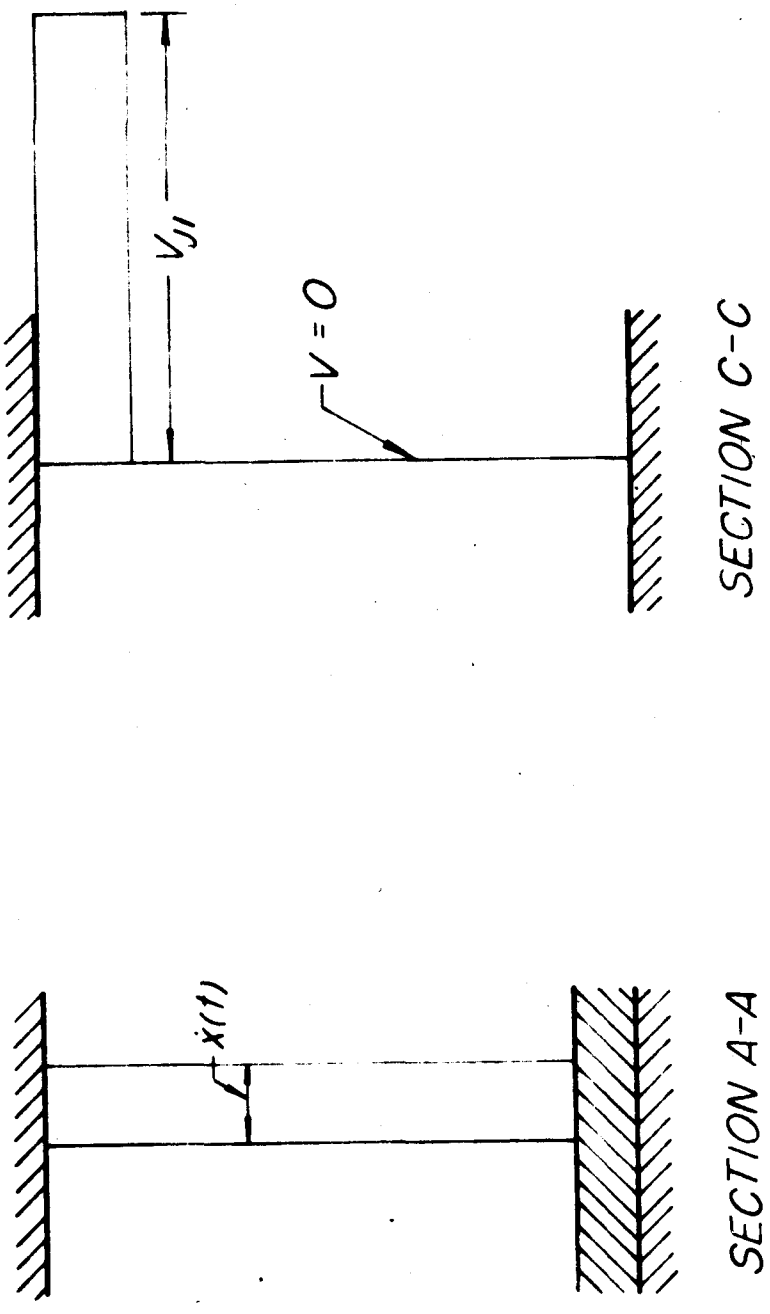

Fig. 4B. Velocities at different sections for the second phase in the analysis, (x(t) > 2.75 inches)

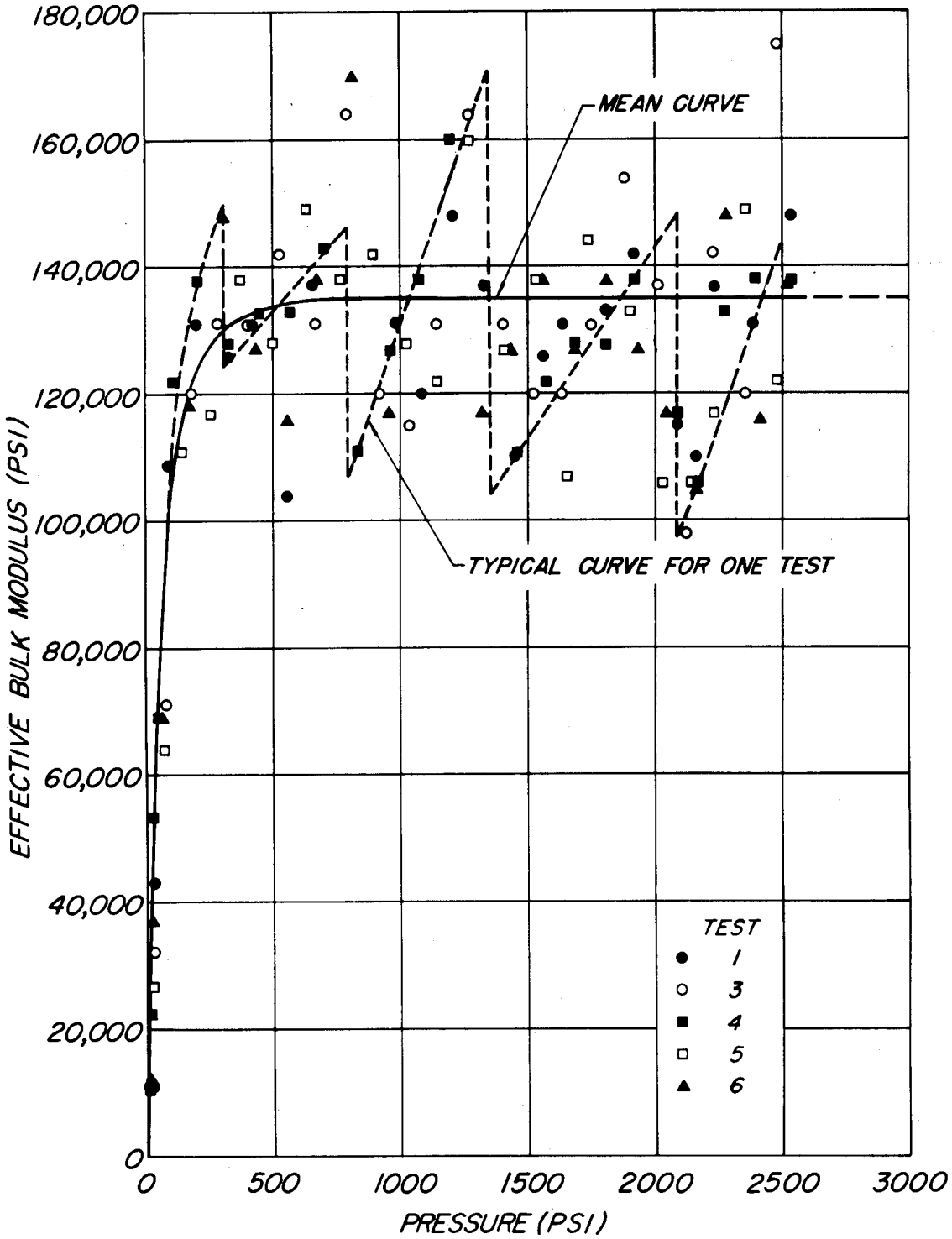

Fig. 5. Effective bulk modulus by pumping tests on the M140 Recoil Mechanism at the Rock Island Arsenal

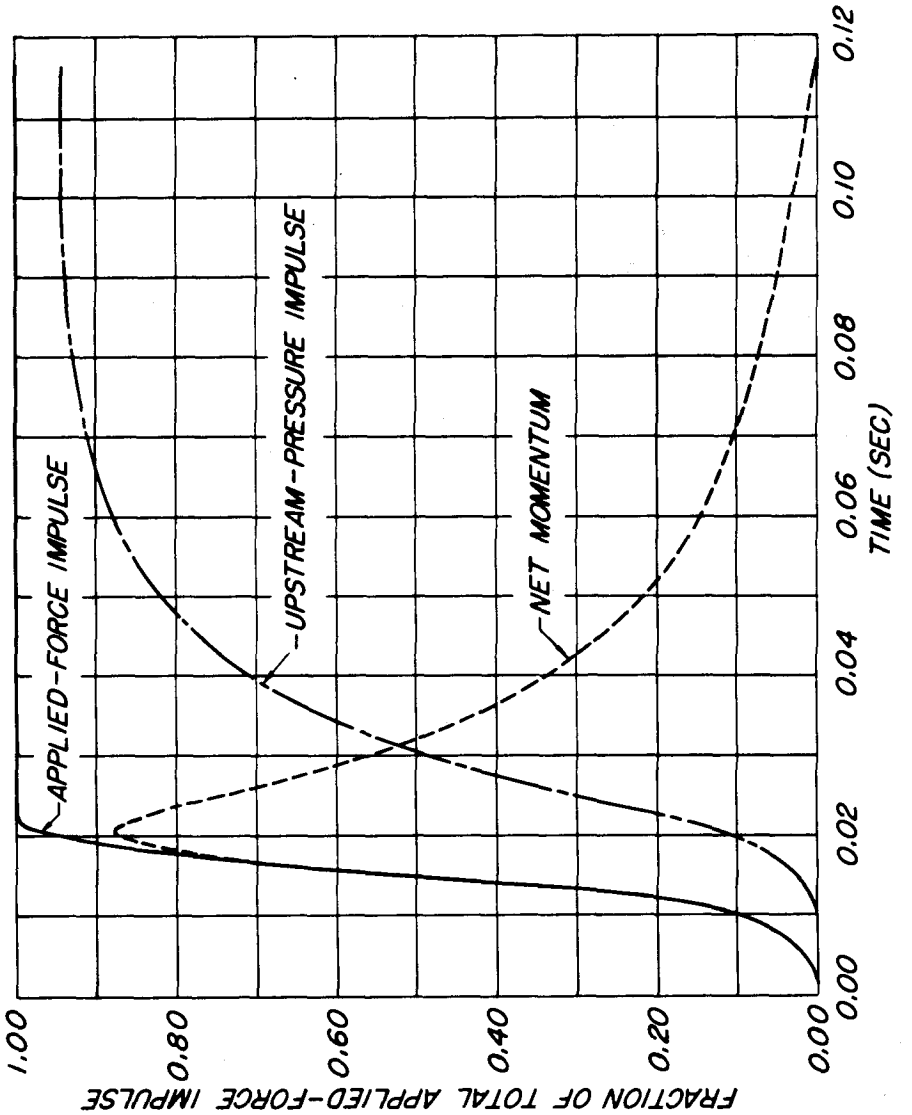

Fig. 6. Momentum-Impulse balance in the M140 recoil mechanism, (small terms are given in Fig. 7)

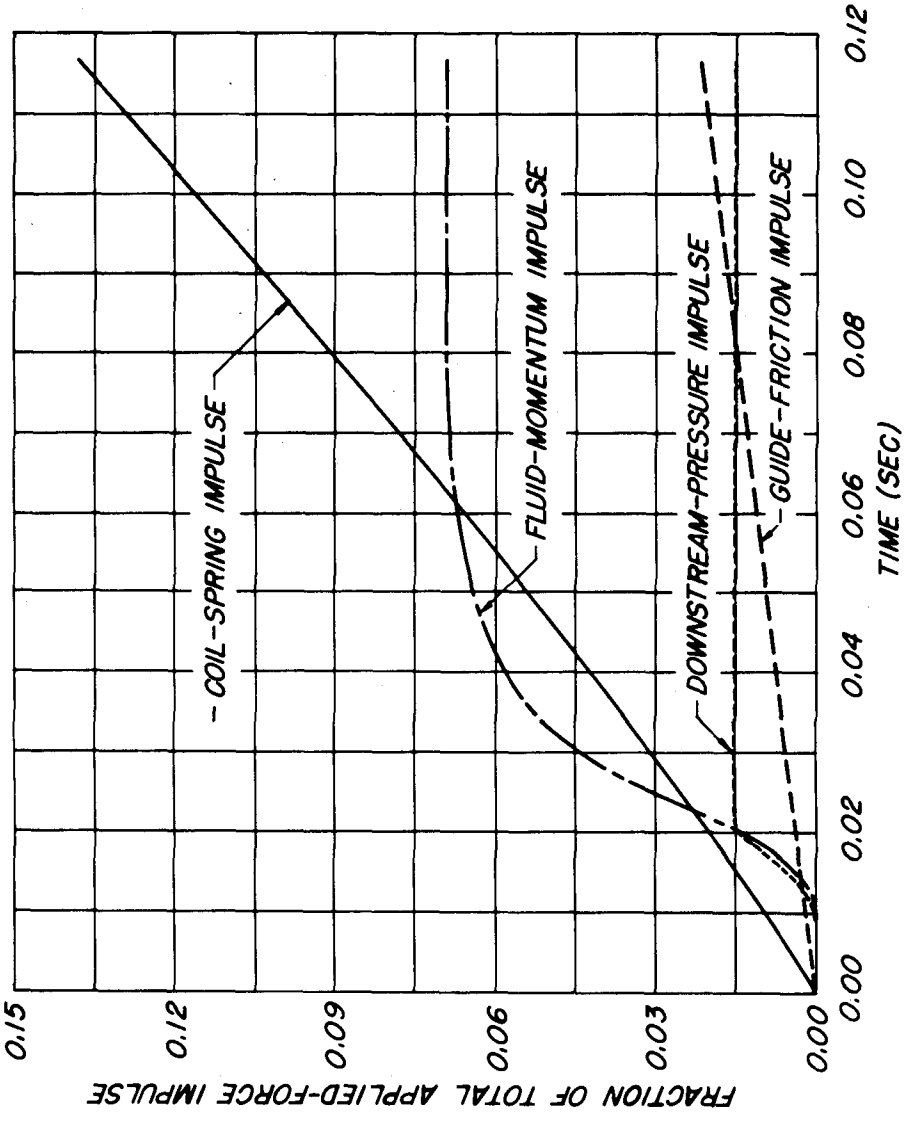

Fig. 7. Impulse of different forces

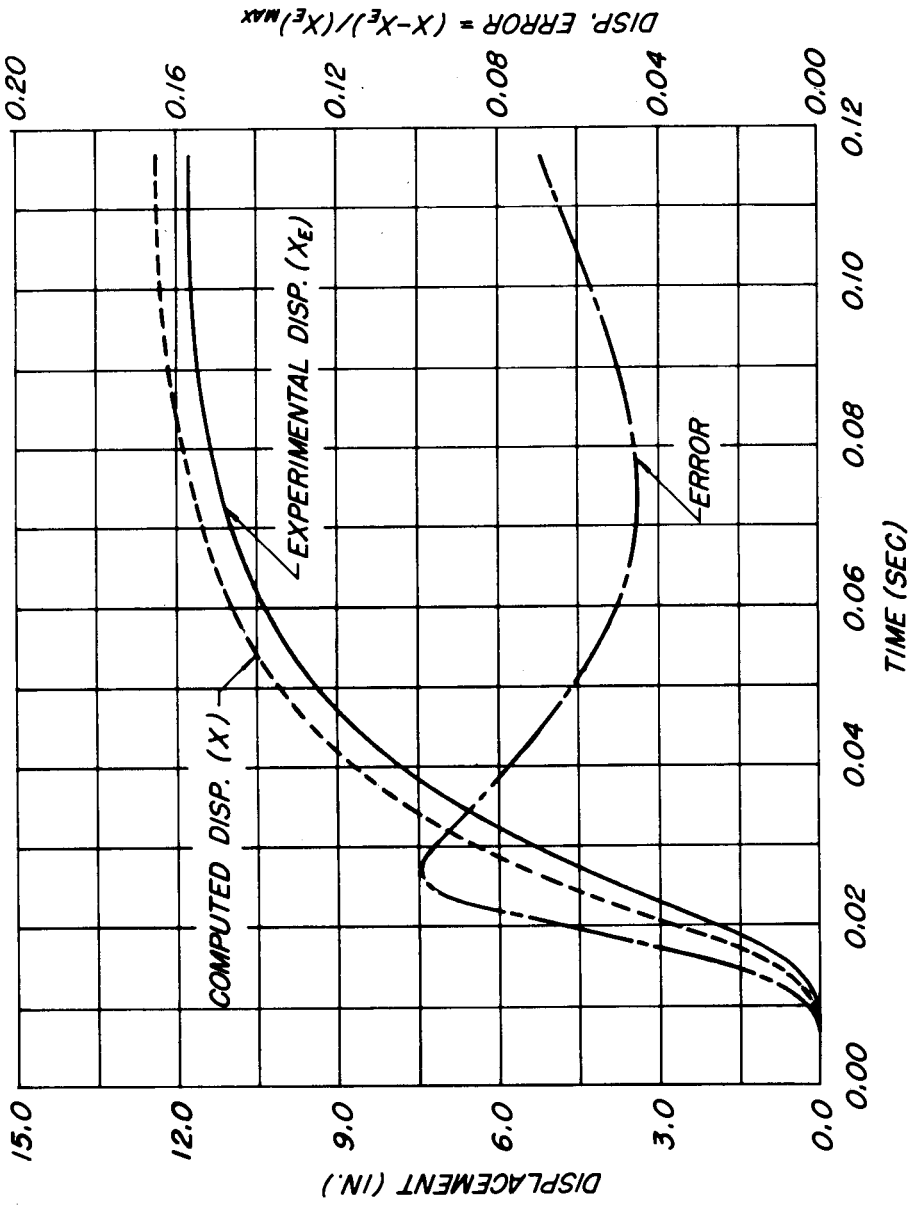

Fig. 8. Comparison of computed and experimentally determined displacement for the standard run

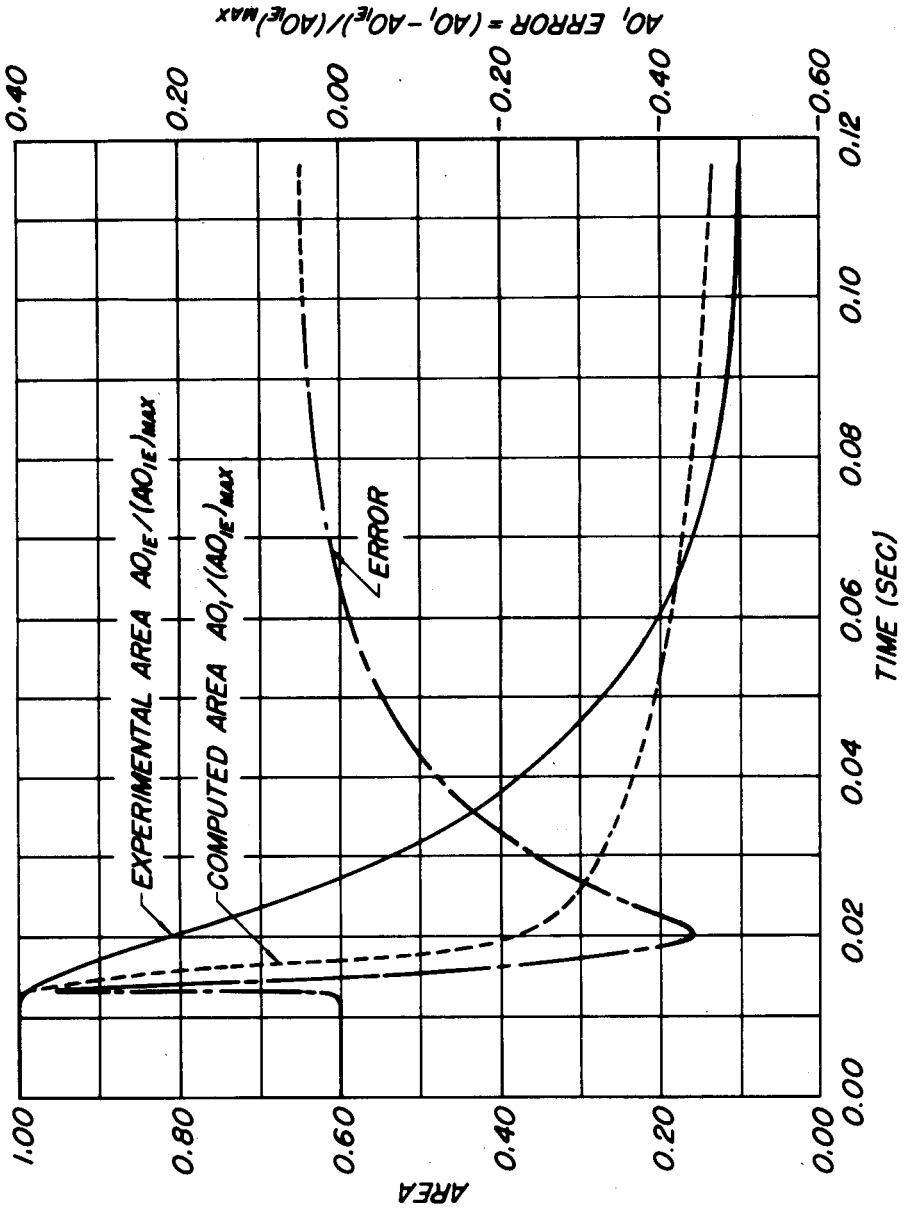

Fig. 9. Comparison of experimental and computed orifice area

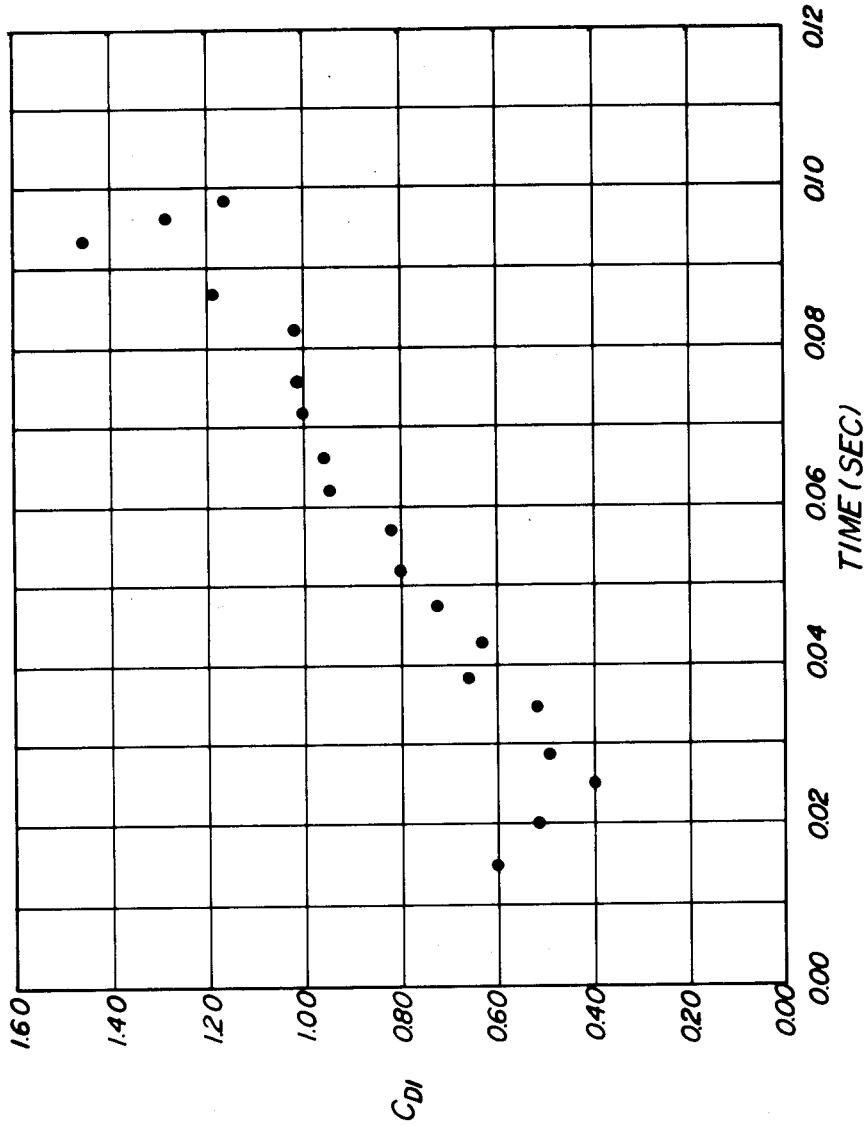

Fig. 10. Calculated values of the discharge coefficient

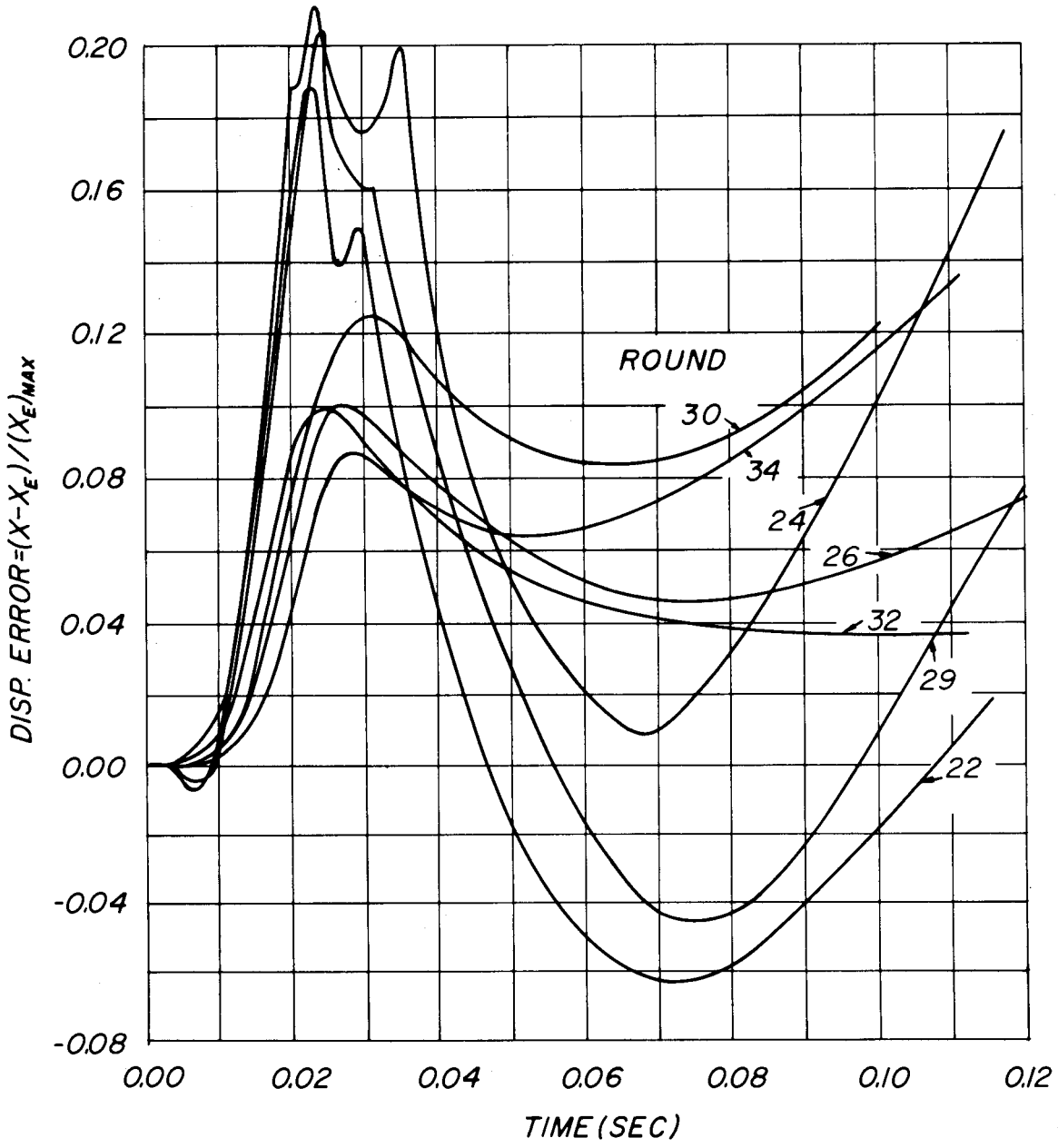

Fig. 11. Comparison of the deviations in the displacement for the different rounds

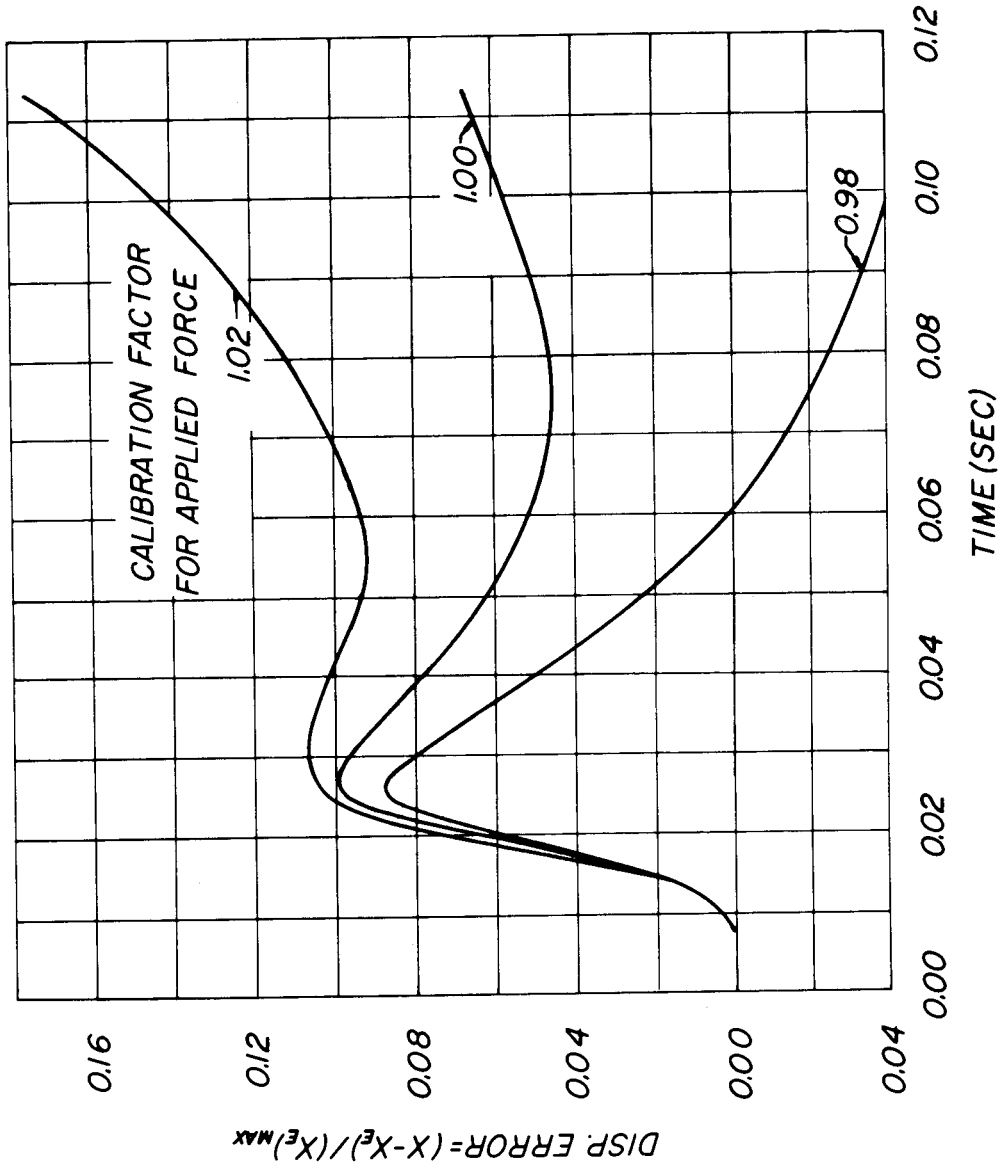

Fig. 12. Effect of variations of the calibration factor for the applied force

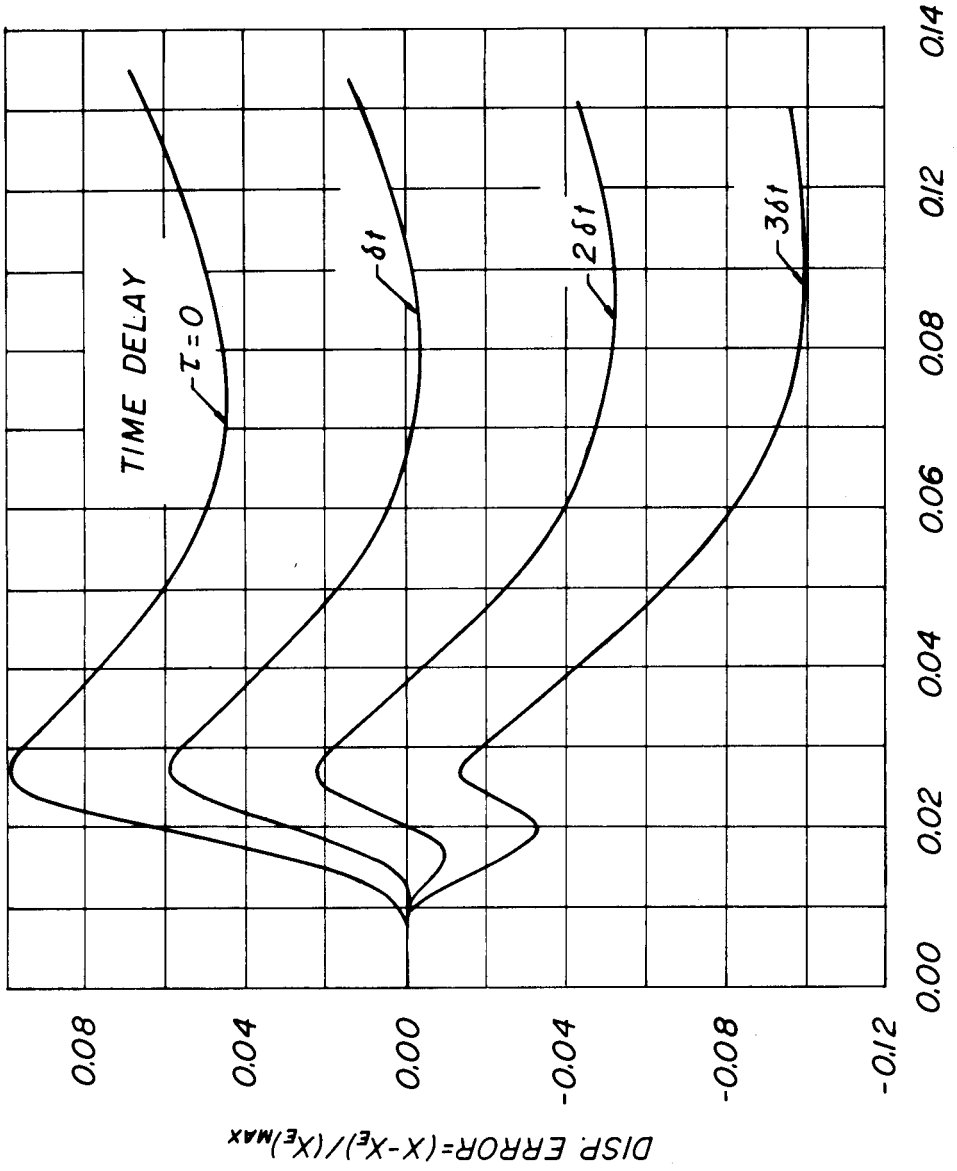

Fig. 13. Influence of time delay of the applied force on the displacement error

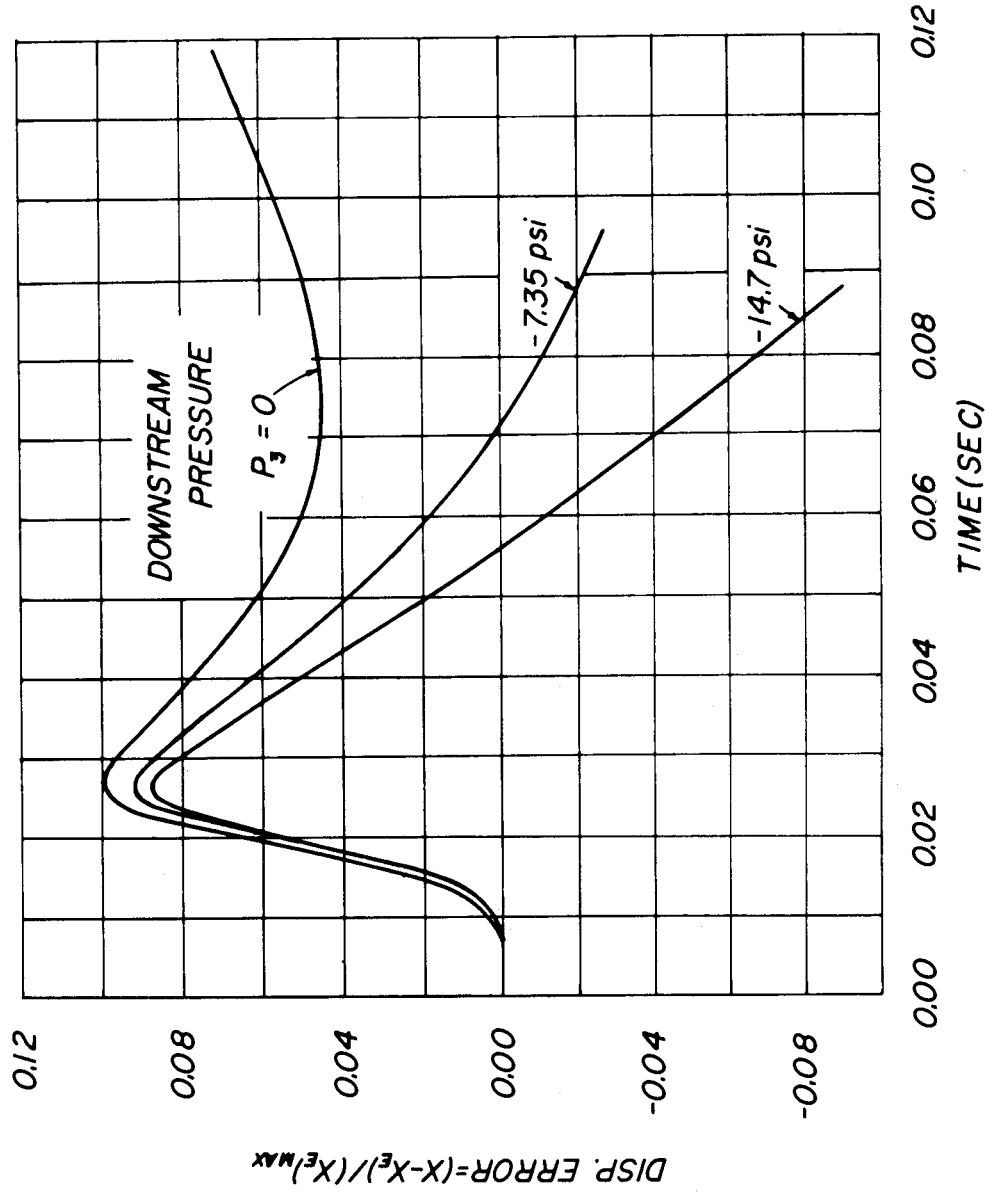

Fig. 14. Influence of the value of the downstream pressure on the displacement error

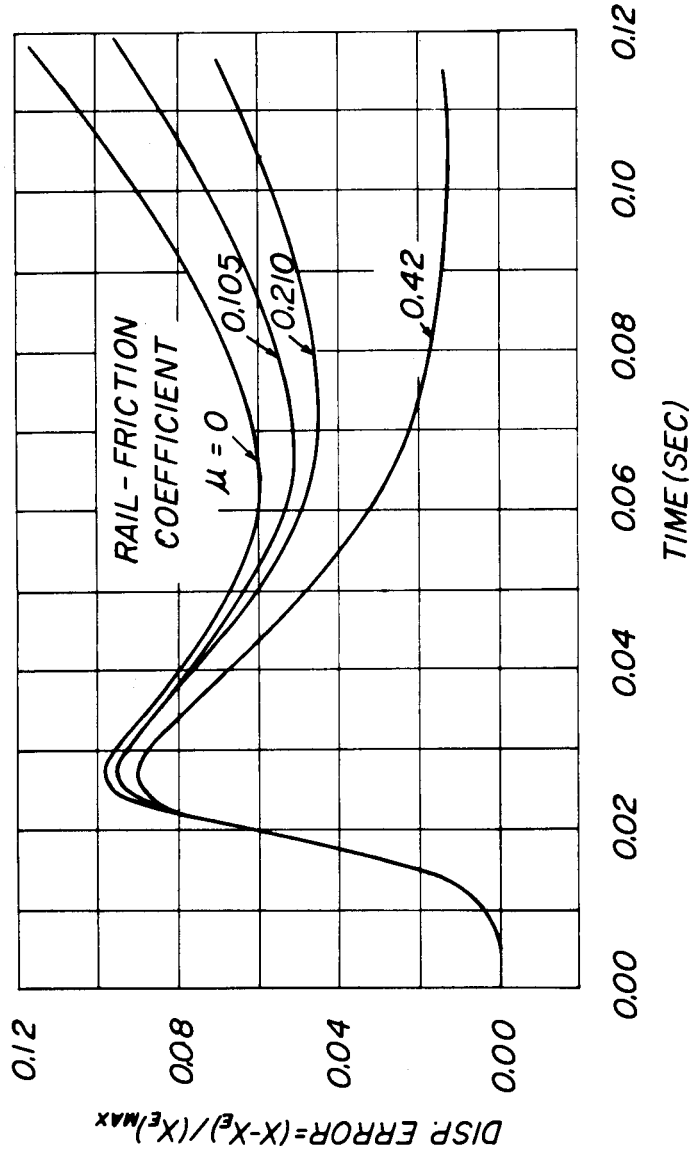

Fig. 15. Influence of the assumed rail coefficient on the displacement error

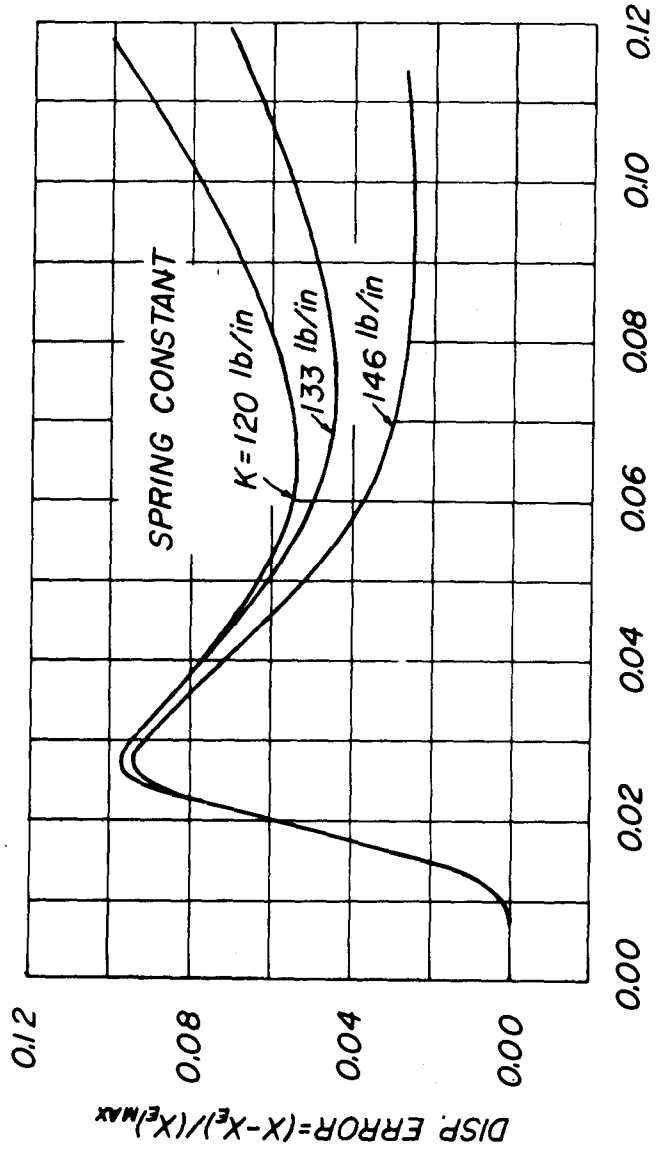

Fig. 16. Influence of the spring constant on the displacement error

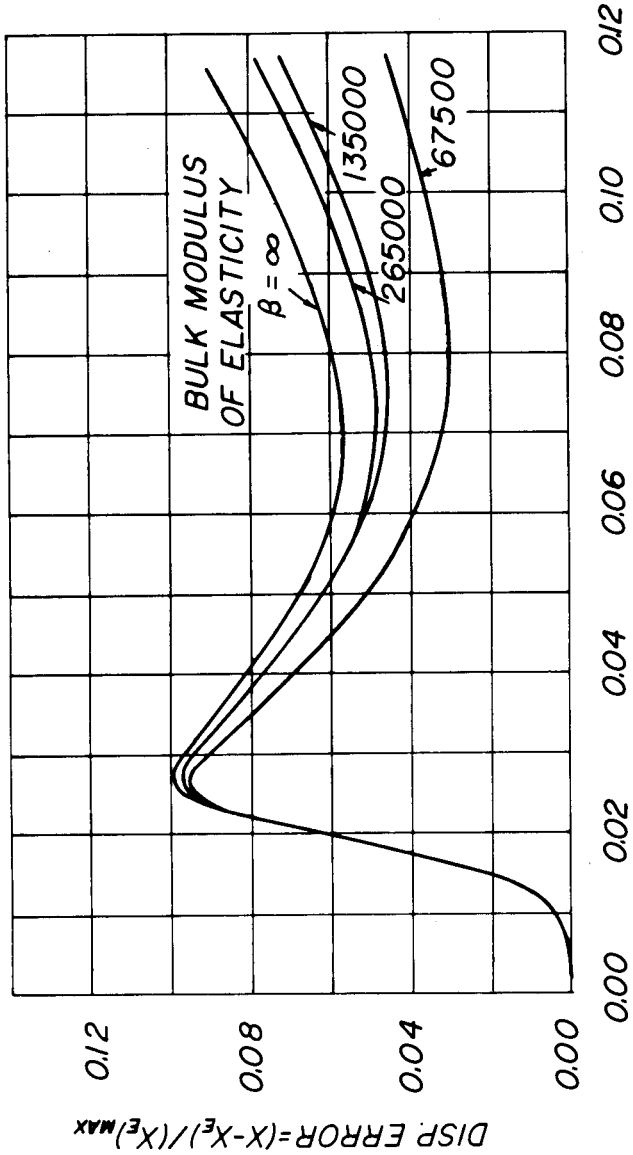

Fig. 17. Influence of different values of the bulk modulus of elasticity on the displacement error

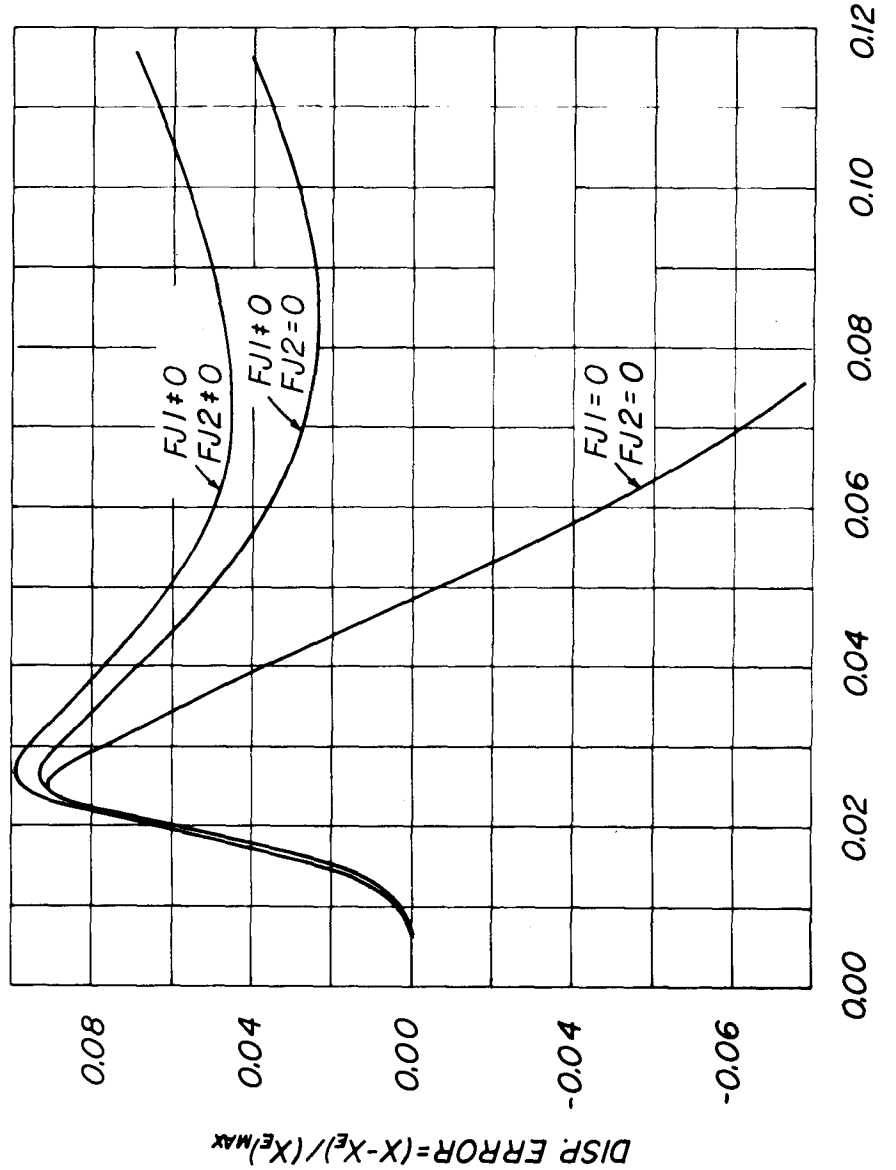

Fig. 18. Influence of different assumptions on the reactions of internal jets on the displacement error

Appendix A

COMPUTER PROGRAM

Numerical Technique

In the analysis of the XM37 recoil mechanism [1], computations were conducted to determine acceleration, velocity, displacement and pressure for a prescribed orifice area. For the M140 recoil mechanism, the computational procedure has been reversed in the sense that the upstream pressure is given and the acceleration, the velocity, the displacement and the orifice area at section 1 are computed. In the present calculations, no numerical instability has been encountered, while for the XM37-recoil-mechanism study, numerical instability arose in the determination of pressure. The improved numerical stability found for this case may be due to using the pressure rather than the orifice area as one of the prescribed variables.

The numerical solution for the computed acceleration, velocity, and displacement is obtained from equation of motion of the recoiling parts (Eqs. 42 and 43); the computations proceed as follows:

1) Read into the computer all necessary data.

2) Assume the acceleration of the recoiling parts and the orifice area at section 1 are equal to the corresponding values at the previous time. Compute the velocity and displacement for the new time by numerical integration using the trapezoidal rule.

3) Calculate the acceleration at the new time with Eq. (42) for $x(t)$ less than 2.75 inches, or with Eq. (43) if $x(t)$ is larger than 2.75 inches.

4) Repeat step 3 at least once, check if the computed displacement and orifice area have converged; if not, repeat step 3 using the latest estimate for acceleration and orifice area. If convergence conditions are satisfied, advance one time-increment, and repeat

steps 2 to 4 until the velocity of the recoiling parts becomes negative.

A detailed description of the computer program is given in the flow charts. The program is written in FORTRAN IV for the IBM 7044 Computer at the University of Iowa Computer Center.

Definition of Terms

A	acceleration of the recoiling parts
A1	area of the normal wall at section 1
A2	area over which P2 is effective
A3	area at section CC (Fig. 3a)
AM	mass of the recoiling parts
AO	mean cross section area in the upstream region
AO1	computed orifice area at the control section 1
AO2	orifice area of control section 2
AO3	computed orifice area at 3
AO1ER	error of control section 1 orifice area
AO1EX	measured orifice area at the control section 1
AO1ST	in-battery orifice area
B	bulk modulus of elasticity of oil
CALF	calibration factor for applied force
CALP1	calibration factor for upstream pressure
CALXE	calibration factor for experimental displacement
CD2, CD3	steady discharge coefficient
CF	coefficient of rail friction
DELT	time interval between computations
DIFF	displacement error
ERR	error for convergence condition
F	applied force
FJ1	jet momentum at section 1
FJ2	jet momentum at section 2
FO	spring force in battery
FS	spring force
JEREAC1	logical statement for setting FJ1 = 0
JEREAC2	logical statement for setting FJ2 = 0
MAXDEL	number of time delay intervals
NEND	maximum number of points computed
NF	number of applied force points read in
NMAX	maximum number of iterations
NP	number of upstream-pressure-data points read in

NR	round number
NRUN	number of runs
NT	number of iterations
NX	number of displacement-data points read in
P1	upstream pressure
P2	pressure at section 2
P3	downstream pressure
Q1	discharge past section 1
Q2	discharge past section 2
Q3	discharge past section 3
QO	equivalent discharge due to the motion of recoiling part
RHO	density of oil
SUMF	applied-force impulse
SUMFJ	sum of jet momentum 1 and 2
SUMFR	sliding-friction impulse
SUMFS	spring-force impulse
SUMP1	upstream-pressure impulse
SUMP23	sum of pressure forces at sections 2 and 3
T	time
TOTIMP	total impulse
V	velocity of the recoiling parts
W	weight of the recoiling parts
X	computed displacement of the recoiling parts
XE	experimental displacement of the recoiling parts
XKS	spring constant
XL1	length of the upstream region in battery
XMOM	momentum of recoiling parts

Flow Chart

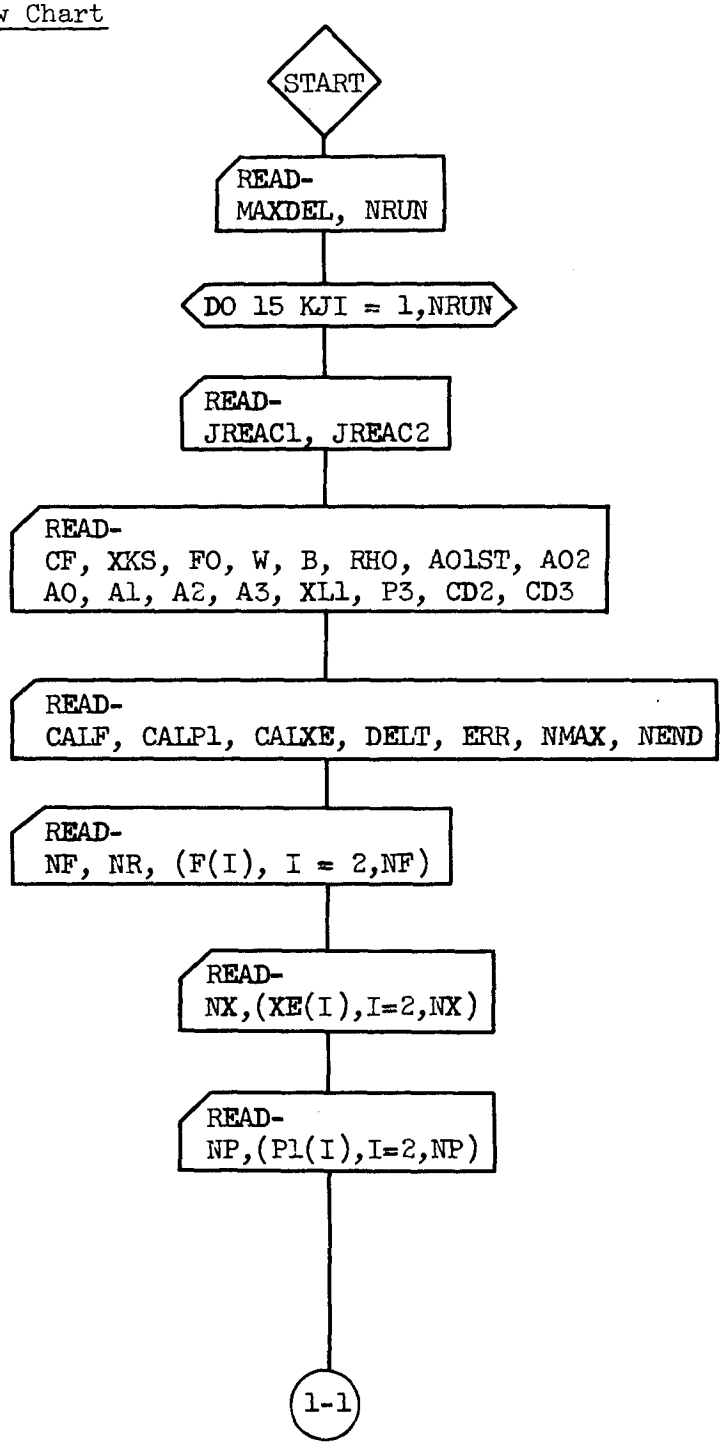

READ NUMBER OF TIME DELAYS AND NUMBER OF RUNS

READ LOGICAL CONTROL OF FLUID MOMENTUM

READ CONSTANTS

READ APPLIED-FORCE DATA

READ MEASURED-DISPLACEMENT DATA

READ UPSTREAM-PRESSURE DATA

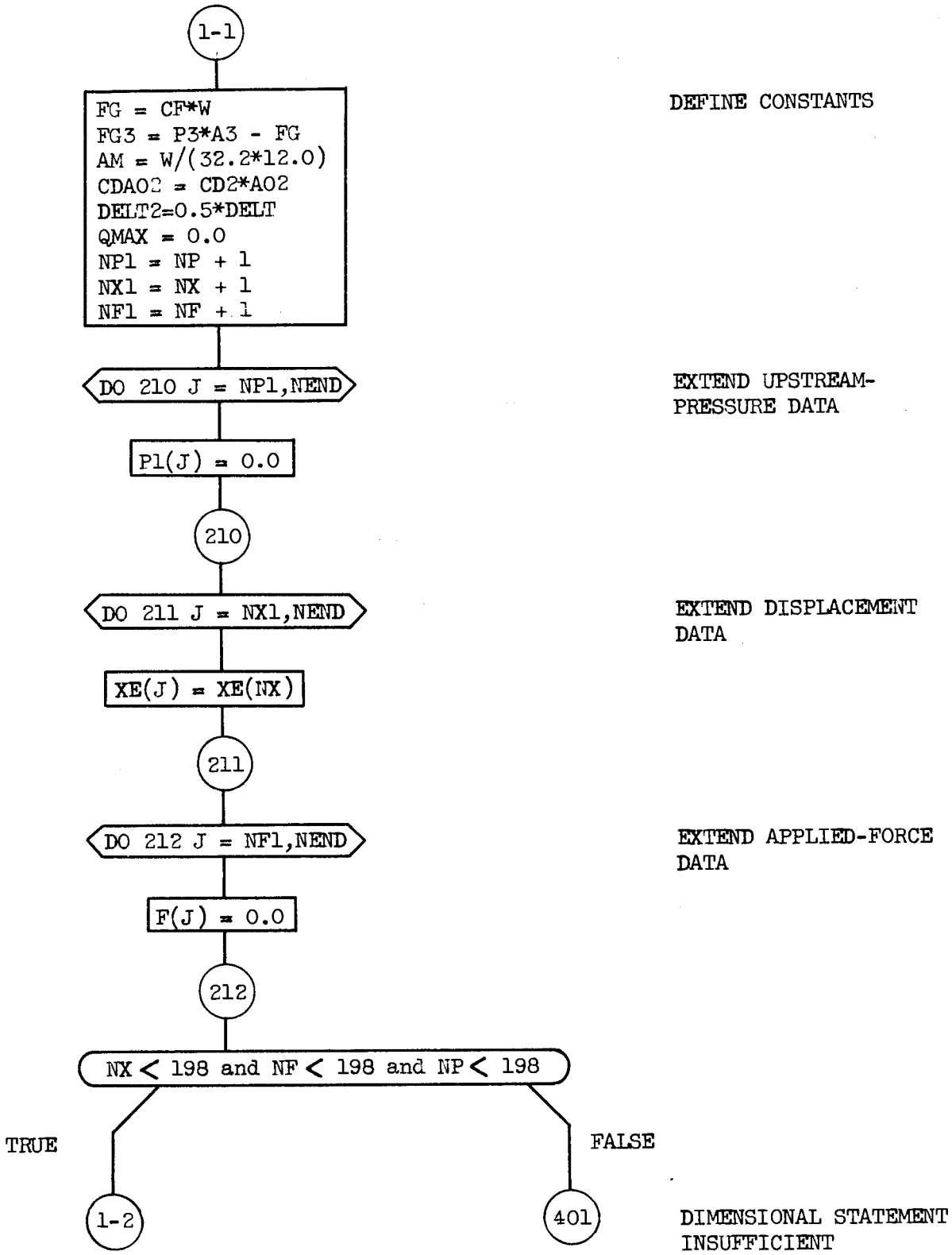
1-1
FG = CF*W
FG3 = P3*A3 - FG
AM = W/(32.2*12.0)
CDA02 = CD2*A02
DELT2=0.5*DELT
QMAX = 0.0
NP1 = NP + 1
NX1 = NX + 1
NF1 = NF + 1
DEFINE CONSTANTS
DO 210 J = NP1,NEND
EXTEND UPSTREAM-PRESSURE DATA
P1(J) = 0.0
210
DO 211 J = NX1,NEND
EXTEND DISPLACEMENT DATA
XE(J) = XE(NX)
211
DO 212 J = NF1,NEND
EXTEND APPLIED-FORCE DATA
F(J) = 0.0
212
NX < 198 and NF < 198 and NP < 198
TRUE
FALSE
1-2
401
DIMENSIONAL STATEMENT INSUFFICIENT

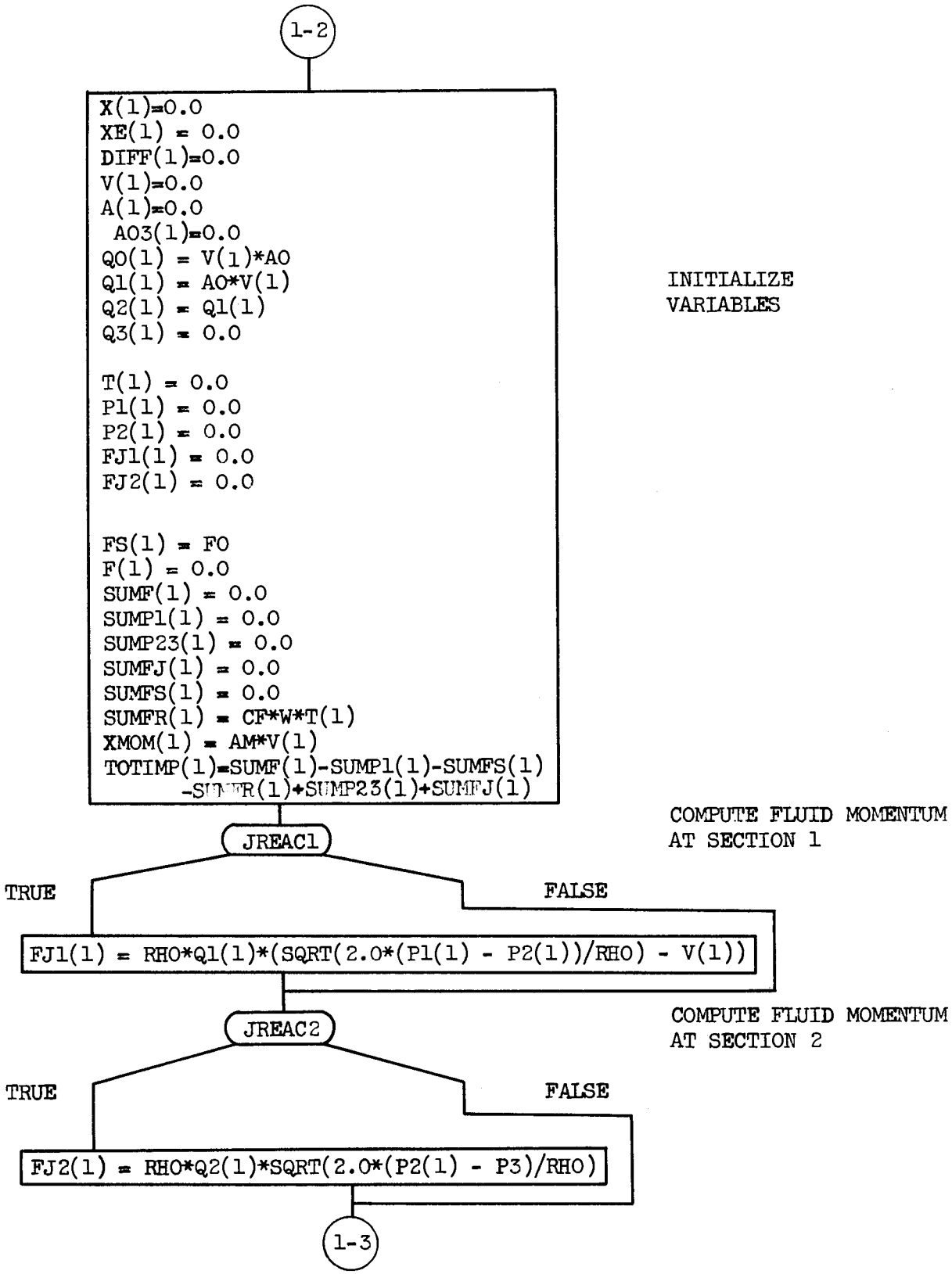
1-2
X(1)=0.0
XE(1) = 0.0
DIFF(1)=0.0
V(1)=0.0
A(1)=0.0
AO3(1)=0.0
QO(1) = V(1)*AO
Q1(1) = AO*V(1)
Q2(1) = Q1(1)
Q3(1) = 0.0
T(1) = 0.0
P1(1) = 0.0
P2(1) = 0.0
FJ1(1) = 0.0
FJ2(1) = 0.0
FS(1) = FO
F(1) = 0.0
SUMF(1) = 0.0
SUMP1(1) = 0.0
SUMP23(1) = 0.0
SUMFJ(1) = 0.0
SUMFS(1) = 0.0
SUMFR(1) = CF*W*T(1)
XMOM(1) = AM*V(1)
TOTIMP(1)=SUMF(1)-SUMP1(1)-SUMFS(1)
-SUMFR(1)+SUMP23(1)+SUMFJ(1)
INITIALIZE VARIABLES
JREAC1
TRUE
FALSE
FJ1(1) = RHO*Q1(1)*(SQRT(2.0*(P1(1) - P2(1))/RHO) - V(1))
COMPUTE FLUID MOMENTUM AT SECTION 1
JREAC2
TRUE
FALSE
FJ2(1) = RHO*Q2(1)*SQRT(2.0*(P2(1) - P3)/RHO)
COMPUTE FLUID MOMENTUM AT SECTION 2
1-3

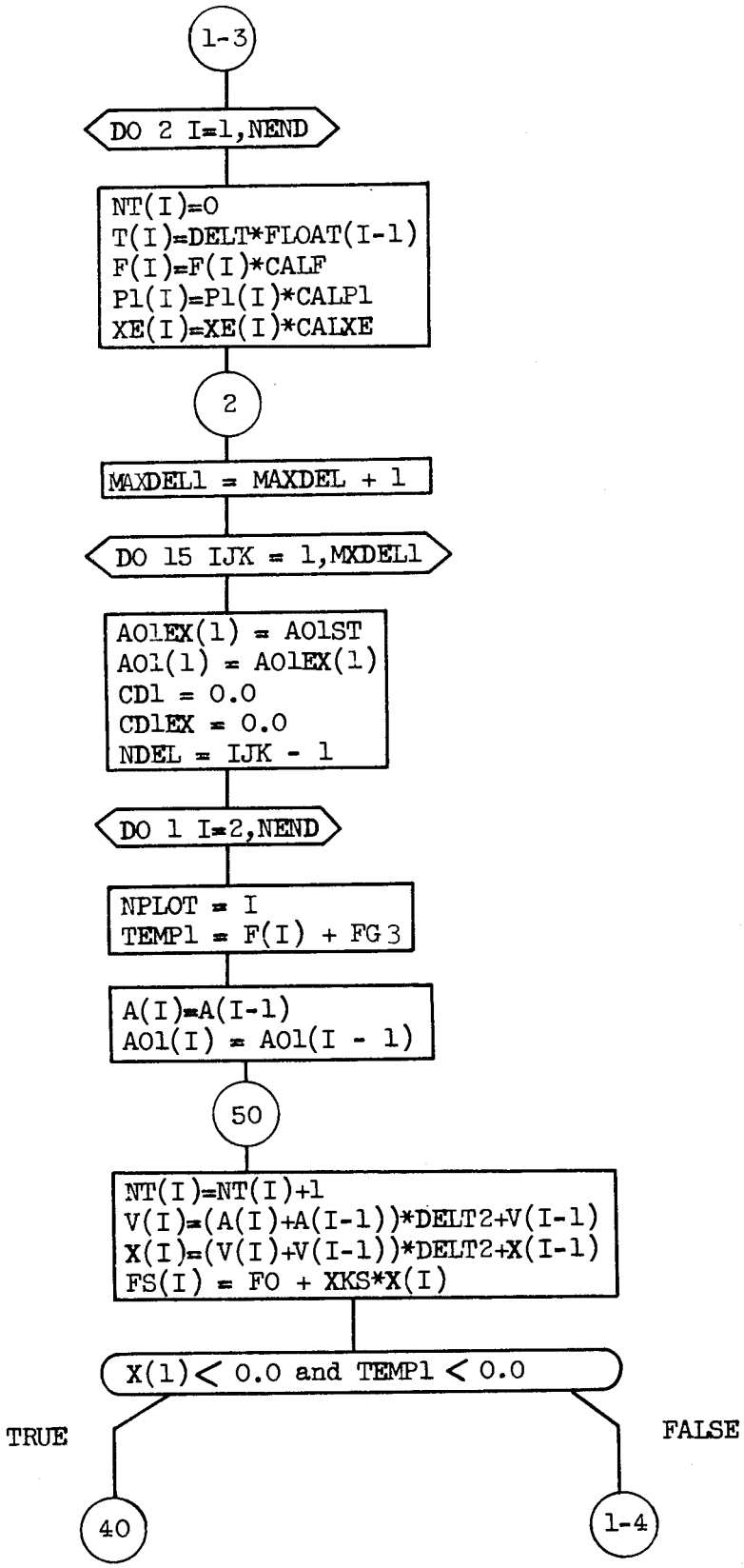

COMPUTE TIME, FORCE PRESSURE AND DISPLACEMENT FOR A COMPLETE RUN

PERFORM ADDITIONAL CYCLES IF TIME DELAYS ARE DESIRED

PERFORM COMPUTATION FOR ONE RUN

ESTIMATE ACCELERATION AND ORIFICE AREA 1

COMPUTE VELOCITY, DISPLACEMENT AND SPRING FORCE

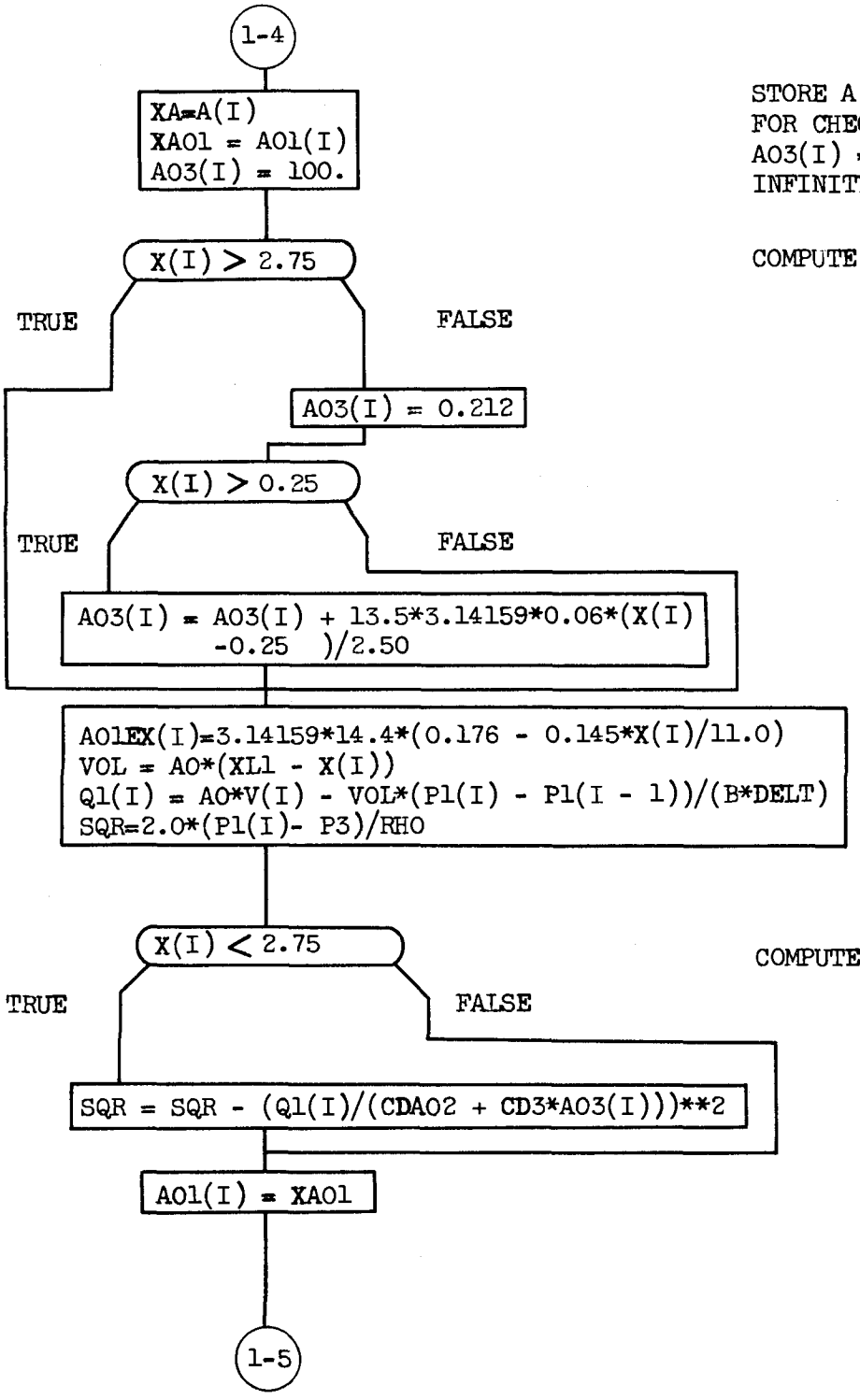

STORE A(t) AND AO1(t) FOR CHECKING CONVERGENCE AO3(I) = 100. REPRESENTS INFINITY

COMPUTE ORIFICE AREA 3

COMPUTE ORIFICE AREA 1

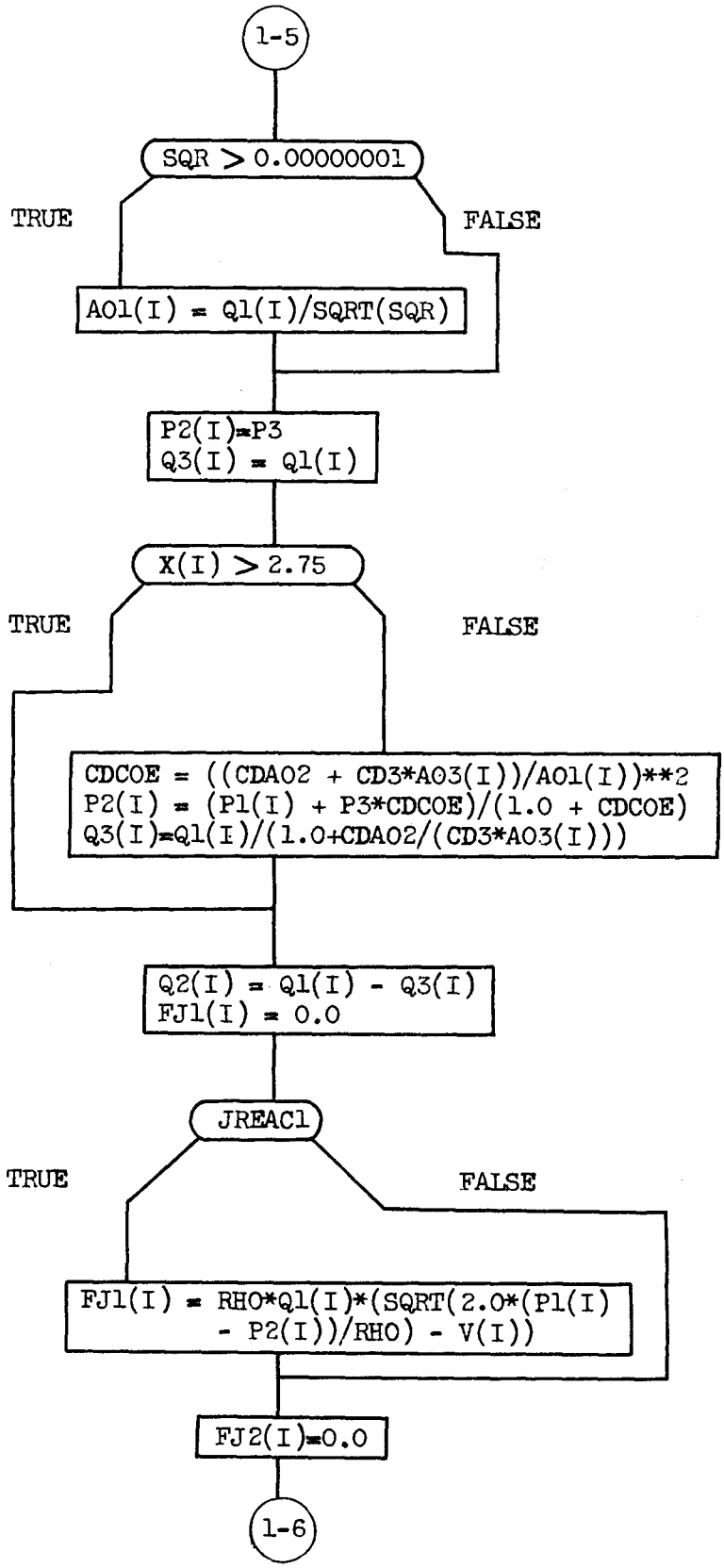

COMPUTE P2(t) AND Q3(t)

COMPUTE Q2(t) AND FLUID-MOMENTUM AT SECTION 1 AND 2

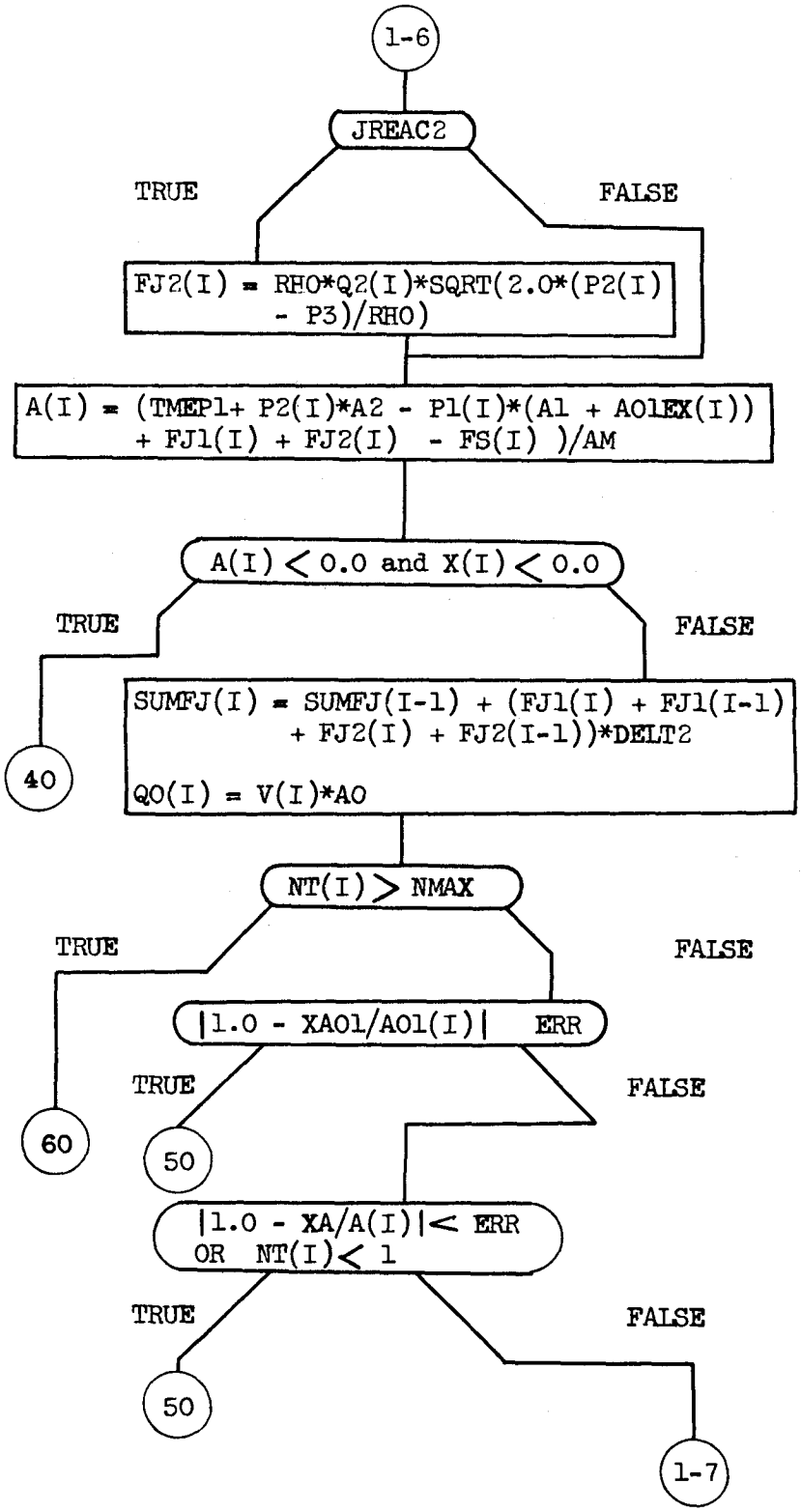
1-6
JREAC2
TRUE
FALSE
FJ2(I) = RHO*Q2(I)*SQRT(2.0*(P2(I) - P3)/RHO)
A(I) = (TMEP1+ P2(I)*A2 - P1(I)*(A1 + AO1EX(I)) + FJ1(I) + FJ2(I) - FS(I))/AM
COMPUTE ACCELERATION A(t)
A(I) < 0.0 and X(I) < 0.0
TRUE
FALSE
40
SUMFJ(I) = SUMFJ(I-1) + (FJ1(I) + FJ1(I-1) + FJ2(I) + FJ2(I-1))*DELT2
QO(I) = V(I)*AO
NT(I) > NMAX
TRUE
FALSE
|1.0 - XAO1/AO1(I)| ERR
CHECK CONVERGENCE CONDITION ON ACCELERATION AND ORIFICE AREA
TRUE
FALSE
60
50
|1.0 - XA/A(I)|< ERR OR NT(I)< 1
TRUE
FALSE
50
1-7

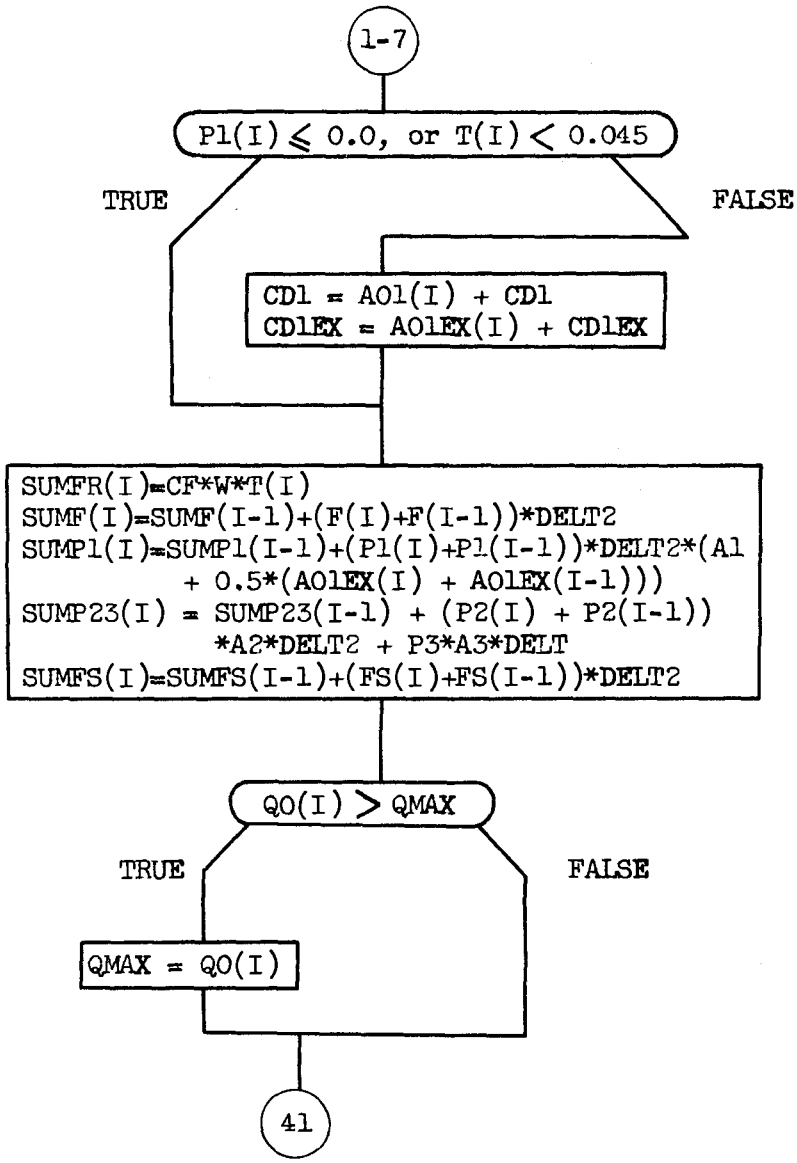

OBTAIN AVERAGE DISCHARGE COEFFICIENT

INTEGRATE FORCES WITH RESPECT TO TIME TO OBTAIN IMPULSIVE TERMS

FIND GREATEST VALUE OF QO(t)

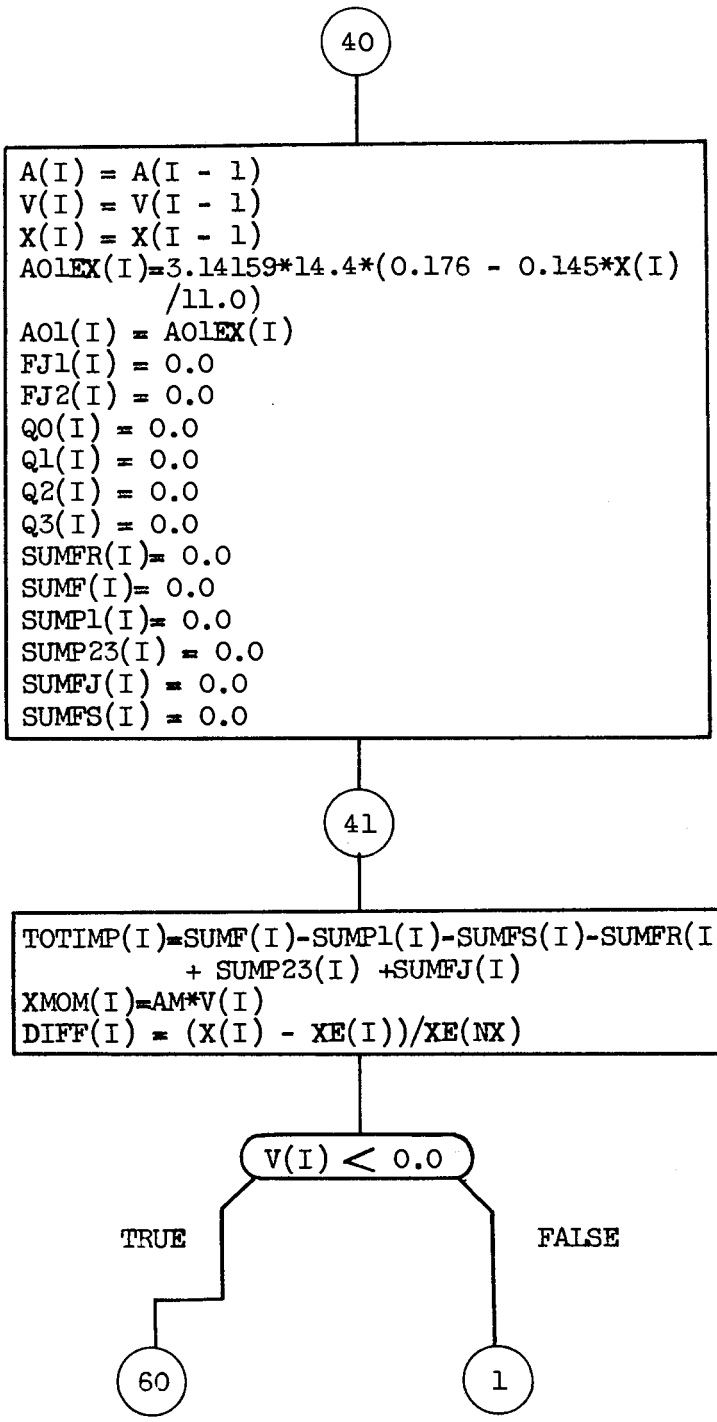

IF A(t) AND X(t) ARE NEGATIVE, OR ZERO (NO NEGATIVE DISPLACEMENT CONDITION)

COMPUTE TOTAL IMPULSE AND NET MOMENTUM

IF VELOCITY LESS THAN ZERO RECOIL STROKE COMPLETED

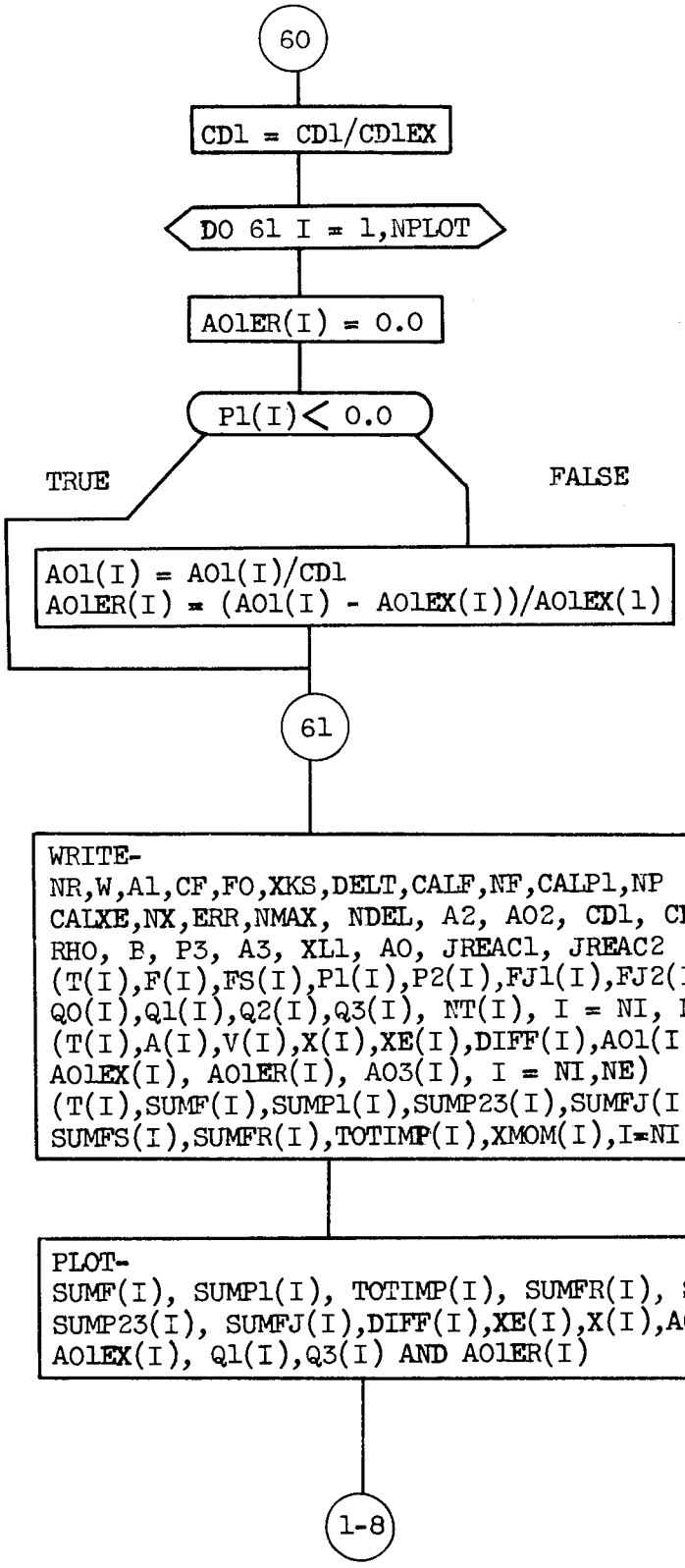

AVERAGE DISCHARGE COEFFICIENT

COMPUTE ORIFICE AREA USING AVERAGE DISCHARGE COEFFICIENT AND ORIFICE-AREA ERROR

PRINT RESULTS

PLOT RESULTS WITH RESPECT TO TIME

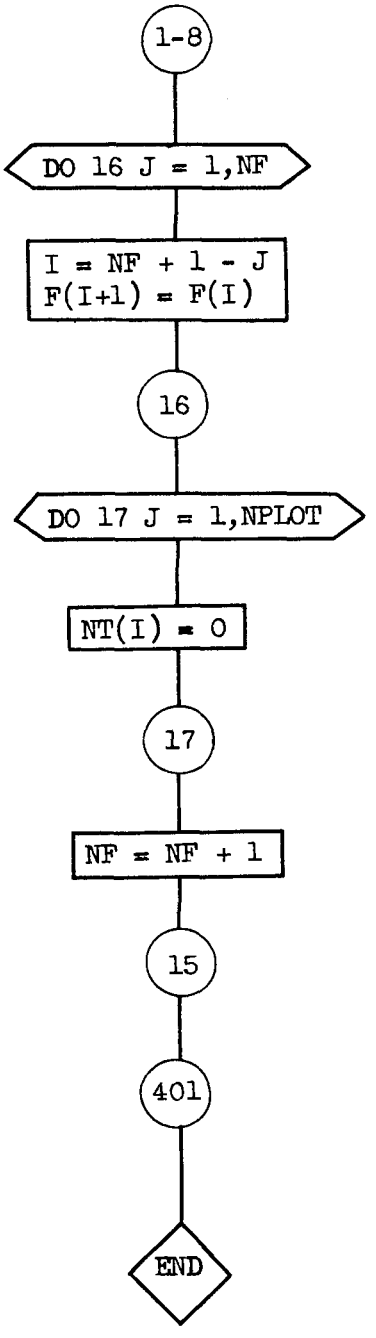

APPLY TIME DELAY
TO APPLIED FORCE

REINITIALIZE ITERATION
COUNT

Computer Program

```
C      M140 RECOIL MECHANISM WITH A MASSLESS SPRING
C      IOWA INSTITUTE OF HYDRAULIC RESEARCH, THE UNIVERSITY OF IOWA

       DIMENSION F(200),P1(200),XE(200),X(200),V(200),A(200),T(200),DIFF(
      1200),NT(200),FS(200),SUMFR(200),SUMF(200),SUMP1(200),SUMFS(200),XM
      2OM(200),TOTIMP(200), AO1(200), AO3(200), P2(200), SUMP23(200),
      3AO1ER(200),AO1EX(200),Q1(200), Q2(200), Q3(200), FJ1(200), FJ2(200
      4),          SUMFJ(200), Q0(200)
       LOGICAL JREAC1, JREAC2
       READ(5,2000) MAXDEL, NRUN
 2000 FORMAT(2I5)
       DO 15 KJI = 1,NRUN
       READ(5,100)      CF, XKS, FO, W, B, RHO, JREAC1, JREAC2
  100 FORMAT(6F10.5, 2L5)
       READ(5,101) A0, A1, A2, A3, XL1, P3,       CD2, CD3, AO1ST, AO2
  101 FORMAT(6F10.5/1F20.5, 3F10.5)
       READ(5,102) CALF, CALP1, CALXE, DELT, ERR, NMAX, NEND
  102 FORMAT(3F10.3, 2F10.8,2I5)
       READ(5,201) NF, NR, (F(I), I = 2,NF)
  201 FORMAT (I5, 1I10/(5F10.5))
       READ (5,200) NX,(XE(I),I=2,NX)
       READ (5,200) NP,(P1(I),I=2,NP)
  200 FORMAT (I5/(5F10.5))
       FG = CF*W
       FG3 = P3*A3 - FG
       AM = W/(32.2*12.0)
       CDAO2 = CD2*AO2
       DELT2=0.5*DELT
       QMAX = 0.0
       NP1 = NP + 1
       NX1 = NX + 1
       NF1 = NF + 1
       DO 210 J = NP1,NEND
  210 P1(J) = 0.0
       DO 211 J = NX1,NEND
  211 XE(J) = XE(NX)
       DO 212 J = NF1,NEND
  212 F(J) = 0.0
       IF (NX.LT.198.AND.NF.LT.198.AND.NP.LT.198) GO TO 3
       WRITE (6,301)
  301 FORMAT (50H NUMBER OF POINTS GREATER THAN DIMENSION STATEMENT)
       GO TO 401
C      INITIALISE VARIABLES
    3  X(1)=0.0
       XE(1) = 0.0
       DIFF(1)=0.0
       V(1)=0.0
       A(1)=0.0
        AO3(1)=0.0
       Q0(1) = V(1)*A0
       Q1(1) = A0*V(1)
```

```
      Q2(1) = Q1(1)
      Q3(1) = 0.0
      T(1) = 0.0
      P1(1) = 0.0
      P2(1) = 0.0
      FJ1(1) = 0.0
      FJ2(1) = 0.0
      IF(JREAC1) FJ1(1) = RHO*Q1(1)*(SQRT(2.0*(P1(1) - P2(1))/RHO) - V(1
     1))
      IF(JREAC2) FJ2(1) = RHO*Q2(1)*SQRT(2.0*(P2(1) - P3)/RHO)
      FS(1) = FO
      F(1) = 0.0
      SUMF(1) = 0.0
      SUMP1(1) = 0.0
      SUMP23(1) = 0.0
      SUMFJ(1) = 0.0
      SUMFS(1) = 0.0
      SUMFR(1) = CF*W*T(1)
      XMOM(1) = AM*V(1)
      TOTIMP(1)=SUMF(1)-SUMP1(1)-SUMFS(1)-SUMFR(1) + SUMP23(1) +SUMFJ(1)
      DO 2 I=1,NEND
      NT(I)=0
      T(I)=DELT*FLOAT(I-1)
      F(I)=F(I)*CALF
      P1(I)=P1(I)*CALP1
    2 XE(I)=XE(I)*CALXE
      MXDEL1 = MAXDEL + 1
      DO 15 IJK = 1,MXDEL1
      AO1EX(1) = AO1ST
      AO1(1) = AO1EX(1)
      CD1 = 0.0
      CD1EX = 0.0
      NDEL = IJK - 1
      DO 1 I=2,NEND
      NPLOT = I
      TEMP1 = F(I) + FG3
      A(I)=A(I-1)
      AO1(I) = AO1(I - 1)
   50 NT(I)=NT(I)+1
      V(I)=(A(I)+A(I-1))*DELT2+V(I-1)
      X(I)=(V(I)+V(I-1))*DELT2+X(I-1)
      FS(I) = FO + XKS*X(I)
      IF(X(I) .LE. 0.0 .AND. TEMP1 .LE. 0.0  ) GO TO 40
      XA=A(I)
      XAO1 = AO1(I)
      AO3(I) = 100.
      IF(X(I) .GT. 2.75) GO TO 6
      AO3(I) = 0.212
      IF(X(I) .GT. 0.25) AO3(I) = AO3(I) + 13.5*3.14159*0.06*(X(I) -0.25
     1)/2.50
    6 AO1EX(I)=3.14159*14.4*(0.176 - 0.145*X(I)/11.0)
      VOL = AO*(XL1 - X(I))
      Q1(I) = AO*V(I) - VOL*(P1(I) - P1(I - 1))/(B*DELT)
      SQR=2.0*(P1(I)- P3)/RHO
      IF(X(I) .LT. 2.75) SQR = SQR - (Q1(I)/(CDAO2 + CD3*AO3(I)))**2
```

```
      AO1(I) = XAO1
      IF(SQR .GT. 0.00000001)  AO1(I) = Q1(I)/SQRT(SQR)
      P2(I)=P3
      Q3(I) = Q1(I)
      IF(X(I).GT.2.75) GO TO 49
      CDCOE = ((CDAO2 + CD3*AO3(I))/AO1(I))**2
      P2(I) = (P1(I) + P3*CDCOE)/(1.0 + CDCOE)
      Q3(I)=Q1(I)/(1.0+CDAO2/(CD3*AO3(I)))
   49 Q2(I) = Q1(I) - Q3(I)
      FJ1(I) = 0.0
      IF(JREAC1) FJ1(I) = RHO*Q1(I)*(SQRT(2.0*(P1(I) - P2(I))/RHO)- V(I)
     1)
      FJ2(I)=0.0
      IF(JREAC2) FJ2(I) = RHO*Q2(I)*SQRT(2.0*(P2(I) - P3)/RHO)
      A(I) = (TEMP1+ P2(I)*A2 - P1(I)*(A1 + AO1EX(I)) + FJ1(I) + FJ2(I)
     1 - FS(I) )/AM
      IF(A(I) .LT. 0.0 .AND. X(I) .LE. 0.0) GO TO 40
      SUMFJ(I) = SUMFJ(I-1) + (FJ1(I) + FJ1(I-1) + FJ2(I) + FJ2(I-1))*DE
     1LT2
      Q0(I) = V(I) *A0
      IF (NT(I).GT.NMAX) GO TO 60
      IF(ABS(1.0 - XAO1/AO1(I)) .GT. ERR) GO TO 50
      IF(ABS(1.0 - XA/A(I)) .GT. ERR .OR. NT(I) .LE. 1) GO TO 50
      IF(P1(I) .LE. 0.0 .OR. T(I) .LT. 0.045) GO TO 42
      CD1 = AO1(I) + CD1
      CD1EX = AO1EX(I) + CD1EX
   42 SUMFR(I)=CF*W*T(I)
      SUMF(I)=SUMF(I-1)+(F(I)+F(I-1))*DELT2
      SUMP1(I)=SUMP1(I-1)+(P1(I)+P1(I-1))*DELT2*(A1 + 0.5*(AO1EX(I) +
     1AO1EX(I-1)))
      SUMP23(I) = SUMP23(I-1) + (P2(I) + P2(I-1))*A2*DELT2 + P3*A3*DELT
      SUMFS(I)=SUMFS(I-1)+(FS(I)+FS(I-1))*DELT2
      IF(Q0(I) .GT. QMAX) QMAX = Q0(I)
      GO TO 41
   40 A(I) = A(I - 1)
      V(I) = V(I - 1)
      X(I) = X(I - 1)
      AO1EX(I)=3.14159*14.4*(0.176 - 0.145*X(I)/11.0)
      AO1(I) = AO1EX(I)
      FJ1(I) = 0.0
      FJ2(I) = 0.0
      Q0(I) = 0.0
      Q1(I) = 0.0
      Q2(I) = 0.0
      Q3(I) = 0.0
      SUMFR(I)=  0.0
      SUMF(I)=  0.0
      SUMP1(I)=  0.0
      SUMP23(I) = 0.0
      SUMFJ(I) = 0.0
      SUMFS(I)  = 0.0
   41 TOTIMP(I)=SUMF(I)-SUMP1(I)-SUMFS(I)-SUMFR(I) + SUMP23(I) +SUMFJ(I)
      XMOM(I)=AM*V(I)
      DIFF(I) = (X(I) - XE(I))/XE(NX)
      IF(V(I).LT.0.0) GO TO 60
```

```
  1 CONTINUE
 60 CD1 = CD1/CD1EX
    DO 61 I = 1,NPLOT
    AO1ER(I) = 0.0
    IF(P1(I) .LE. 0.0) GO TO 61
    AO1(I) = AO1(I)/CD1
    AO1ER(I) = (AO1(I) - AO1EX(I))/AO1EX(1)
 61 CONTINUE
    WRITE (6,300) NR,W,A1,CF,FO,XKS,DELT,CALF,NF,CALP1,NP
300 FORMAT (1H1,116H  BALANCING MOMENTUM OF M140 RECOIL MECHANISM ASSU
   1MING A STATIC SPRING    BASIC UNITS ARE POUNDS, INCHES AND SECONDS
   2////78H  DATA OBTAINED FROM TESTS PERFORMED ON POWDER GYMNASTICATO
   3R ON APRIL 16, 1965//15H  RND NUMBER = I4//30H  WEIGHT OF RECOILIN
   4G PARTS = F8.0//47H  AREA OVER WHICH PRESSURE, P1, IS EFFECTIVE =
   5F8.3//41H  ASSUMED COEFFICIENT OF RAIL FRICTION = F8.3//42H  SPRIN
   6G      FORCE IN INITIAL POSITION = F8.0/32H                SPRING CO
   7NSTANT = F8.3//18H  TIME INTERVAL = F9.6//25H  CALIBRATION OF FORC
   8E = F8.0, 12X,24HNUMBER OF POINTS READ = I3//28H  CALIBRATION OF P
   9RESSURE =  F7.0,10X,24HNUMBER OF POINTS READ = I3)
    WRITE (6,305)CALXE,NX,ERR,NMAX, NDEL, A2, AO2, CD1, CD2, CD3
305 FORMAT(/   32H  CALIBRATION OF DISPLACEMENT = F6.3, 6X,24H NUMBER
   1OF POINTS READ = I4//40H  ERROR IN ITERATION ON ACCELERATION IS F1
   20.6,18H  OR A MAXIMUM OF I3,12H  ITERATIONS //41H NUMBER OF TIME D
   3ELAYS ON APPLIED FORCE = I5//34H AREA OVER WHICH P2 IS EFFECTIVE =
   4 F8.3//22H AREA OF ORIFICE AO2 =   F7.4//54H DISCHARGE COEF. OF AO
   51, AO2, AND AO3 ARE RESPECTIVELY  3F10.3/)
    WRITE(6,302) RHO, B, P3, A3, XL1, A0, JREAC1, JREAC2
302 FORMAT(21H  DENSITY OF FLUID =  1F10.7,26H, BULK MODULUS OF FLUID
   1=   1F9.0//16H  PRESSURE P3 =   1F6.2,27H AND ACTS OVER AREA (A3)
   2=  1F8.3//39H  INITIAL UPSTREAM REGION (XL1 * A0) =   2F8.3//
   322H  JET REACTIONS FJ1 = 1L3 /15X, 7H FJ2 = 1L3)
    NPE = (NPLOT - 1)/50 + 1
    DO 10 J=1,NPE
    NE=50*J
    NI=NE-49
    IF(NE .GT. NPLOT) NE = NPLOT
    WRITE (6,400) (T(I),F(I),FS(I),P1(I),P2(I),FJ1(I),FJ2(I),
   1 Q0(I),Q1(I),Q2(I),Q3(I), NT(I), I = NI, NE)
400 FORMAT (1H1,125H      TIME    APPLIED       SPRING       P1          P
   12          JET1       JET2                Q0       Q1       Q2        Q
   23       NC/87H                 FORCE         FORCE
   3         FORCE      FORCE           /(1H ,F10.5,2F11.0,2F11.2,2F11.3
   4, 1F19.0, 3F8.0, 1I5))
    WRITE (6,501) (T(I),A(I),V(I),X(I),XE(I),DIFF(I),AO1(I),AO1EX(I),
   1           AO1ER(I), AO3(I), I = NI,NE)
501 FORMAT (1H1,131H       TIME      ACCEL     VELOCITY       COMP
   1   MEAS         DISPL       ORF AO1     ORF AO1                    CD
   21        ORF AO3  /131H                                            DI
   3SP         DISP         ERR         CALC        COMP DISP
   4     ERROR                 /(1H , 1F12.5,1F12.2, 6F12.4, 1F24.4,
   5 1F11.3))
 10 WRITE (6,500) (T(I),SUMF(I),SUMP1(I),SUMP23(I),SUMFJ(I),SUMFS(I),
   1 SUMFR(I),TOTIMP(I),XMOM(I),I=NI,NE)
500 FORMAT (1H1,108H       TIME     APPLIED          P1          P2+P3
   1   JET          SPRING     FRICTION     NET         MOMENTUM/96H
```

```
2              IMPULSE       IMPULSE       IMPULSE    IMPULSE       IMPUL
3SE      IMPULSE      IMPULSE/(1H ,F12.5,F12.2,7F12.4))
  SCLE = SUMF(NPLOT)
  NPL1 = NPLOT + 1
  NPL2 = NPLOT + 2
  T(NPL1) = 0.12
  T(NPL2) = 0.12
  DIFF(NPL1)    = - 0.1
  DIFF(NPL2)    =   0.1
  AO1ER(NPL2) =   0.50
  AO1ER(NPL1) = - 0.50
  Q0(NPL1) =  - 0.1
  Q3(NPL1) =  - 0.1
  Q0(NPL2) = 0.1
  Q3(NPL2) = 0.1
  AO1(NPL1) = 0.0
  AO1EX(NPL1) = 0.0
  AO1EX(NPL2) = 1.0
  AO1(NPL2) = 1.0
  XE(NPL1) = 15.0
   X(NPL1) = 0.0
  DO 5 I = 1,NPL2
5 IF(ABS(DIFF(I)).GT. 0.10) DIFF(I) = 0.1*ABS(DIFF(I))/DIFF(I)
  DO 4 I = 1,NPLOT
  IF(Q0(I) .GT. 0.0) Q3(I) = Q3(I)/Q0(I)
  IF(Q2(I) .LE. 0.0000001) Q3(I) = 0.0
  Q0(I) = (Q0(I) - Q1(I))/QMAX
  AO1EX(I) = AO1EX(I)/AO1ST
  AO1(I) = AO1(I)/AO1ST
  IF(AO1EX(I) .GT. 1.0) AO1EX(I) = 1.0
  IF(AO1(I)   .GT. 1.0) AO1(I)   = 1.0
  IF(ABS(AO1ER(I)) .GT. 0.50) AO1ER(I) = 0.5*ABS(AO1ER(I))/AO1ER(I)
  IF(SUMF(I) .LT. 0.0) SUMF(I) = 0.0
  IF(SUMP1(I) .LT. 0.0) SUMP1(I) = 0.0
  IF (SUMP23(I).LT.0.0) SUMP23(I) = ABS(SUMP23(I))
  IF(SUMFS(I) .LT. 0.0) SUMFS(I) = 0.0
  IF(SUMFR(I) .LT. 0.0) SUMFR(I) = 0.0
  IF(SUMFJ(I) .LT. 0.0) SUMFJ(I) = 0.0
  IF(TOTIMP(I) .LT. 0.0) TOTIMP(I) = 0.0
  IF(ABS(Q0(I)) .GT. 0.10) Q0(I) = 0.1*ABS(Q0(I))/Q0(I)
  IF(ABS(Q3(I)) .GT. 0.10) Q3(I) = 0.1*ABS(Q3(I))/Q3(I)
  IF(ABS(AO1ER(I)) .GT. 0.5) AO1ER(I) = 0.5*ABS(AO1ER(I))/AO1ER(I)
  SUMF(I) = SUMF(I)/SCLE
  SUMP1(I) = SUMP1(I)/SCLE
  SUMP23(I)=SUMP23(I)/SCLE
  SUMFS(I) = SUMFS(I)/SCLE
  SUMFR(I) = SUMFR(I)/SCLE
  SUMFJ(I) = SUMFJ(I)/SCLE
4 TOTIMP(I) = TOTIMP(I)/SCLE
  SUMF(NPL1) = 0.0
  SUMP1(NPL1) = 0.0
  TOTIMP(NPL1) = 0.0
  SUMFR(NPL1) = 0.0
  SUMFS(NPL1) = 0.0
  SUMFJ (NPL1) = 0.0
```

```
      SUMP23(NPL1)=0.15
      WRITE(6,1000) NR, NDEL
 1000 FORMAT( 90H1 TIME VERSUS APPLIED IMPULSE (+), PRESSURE IMPULSE (X)
     1, TOTAL IMPULSE (*), FOR ROUND NO.   I3/45H AND NUMBER OF TIME DEL
     2AYS ON APPLIED FORCE =    I5)
      CALL LPLOT(NPL1, T(1),SUMF(1), SUMP1(1), TOTIMP(1))
      WRITE(6,1002) NR, NDEL
 1002 FORMAT(119H1 TIME VERSUS FRICTION IMPULSE (Y), SPRING IMPULSE (+),
     1, DWN. PRESS. IMPULSE(X), NET FLUID MOMENTUM(*), FOR ROUND NO.
     21I3/45H AND NUMBER OF TIME DELAYS ON APPLIED FORCE =      I5)
      CALL LPLOT(NPL1, T(1), SUMFR(1), SUMFS(1), SUMP23(1), SUMFJ(1))
      WRITE(6,1001) NR, NDEL
 1001 FORMAT(121H1TIME VERSUS DISPLACEMENT  ERROR IN TERMS OF TOTAL RECO
     1IL
     2/ 15H FOR ROUND NO.  1I3, 45H AND NUMBER OF TIME DELAYS ON APPLIED
     3 FORCE =    1I5)
      CALL LPLOT(NPL2, T(1), DIFF(1))
      WRITE(6,1022)
 1022 FORMAT(56H1 EXPERIMENTAL DISPLACEMENT(X), COMPUTED DISPLACEMENT(*)
     1)
      CALL LPLOT(NPL1, T(1), XE(1), X(1))
      WRITE(6,1023)
 1023 FORMAT(56H1 EXPERIMENTAL ORIFICE AREA(*), COMPUTED ORIFICE AREA(X)
     1    )
      CALL LPLOT(NPL2, T(1), AO1(1), AO1EX(1))
      WRITE(6,1024)
 1024 FORMAT(50H1 (Q0 - Q1)/QMAX (X), , AND Q3/Q0(I) (*)                 )
      CALL LPLOT(NPL2, T(1), Q0(1), Q3(1))
      WRITE(6,1025) NR, NDEL
 1025 FORMAT( 53H1 ORIFICE AREA IN TERMS OF IN-BATTERY ORIFICE AREA
     2/ 15H FOR ROUND NO.  1I3, 45H AND NUMBER OF TIME DELAYS ON APPLIED
     3 FORCE =    1I5)
      CALL LPLOT(NPL2, T(1), AO1ER(1))
      DO 16 J = 1,NF
      I = NF + 1 - J
   16 F(I + 1) = F(I)
      DO 17 J = 1,NPLOT
   17 NT(J) = 0
   15 NF = NF + 1
  401 CALL EXIT
      END
```

Security Classification

DOCUMENT CONTROL DATA - R & D

(Security classification of title, body of abstract and indexing annotation must be entered when the overall report is classified)

1. ORIGINATING ACTIVITY (Corporate author)	2a. REPORT SECURITY CLASSIFICATION
Iowa Institute of Hydraulic Research	Unclassified
	2b. GROUP

3. REPORT TITLE

A Preliminary Analysis of the M140 Recoil Mechanism

4. DESCRIPTIVE NOTES (Type of report and inclusive dates)

Technical Report

5. AUTHOR(S) (First name, middle initial, last name)

Arthur D. Newsham, Enzo O. Macagno, and Tin-Kan Hung

6. REPORT DATE	7a. TOTAL NO. OF PAGES	7b. NO. OF REFS
December 1966	77	9

8a. CONTRACT OR GRANT NO.	9a. ORIGINATOR'S REPORT NUMBER(S)
DA-11-070-508-ORD-988	
b. PROJECT NO.	Report No. 100
c.	9b. OTHER REPORT NO(S) (Any other numbers that may be assigned this report)
d.	

10. DISTRIBUTION STATEMENT

Each transmittal of this document outside the Department of Defense must have prior approval of the R. & E. Division, Rock Island Arsenal.

11. SUPPLEMENTARY NOTES	12. SPONSORING MILITARY ACTIVITY
	Rock Island Arsenal

13. ABSTRACT

The equations of motion for the recoil phase of the M140 Recoil Mechanism have been formulated. This mechanism contains a coil spring, the action of which has been represented in a static manner in this preliminary analysis. The system of equations has been solved by reducing it to a system of difference equations. The results of the analysis are compared with data obtained from a series of experiments performed in a powder gymnasticator at the Rock Island Arsenal. The relative effect of the various parameters influencing the motion of the recoiling parts is presented in a systematic manner. A series of graphs show the relative error in the displacement of the recoiling parts of the mechanism due to variations of several parameters. According to the computational model, the effect of deviations in the values of the bulk modulus of elasticity of the hydraulic oil, the spring constant, and the rail-friction coefficient are rather small. On the other hand, the time delay, the downstream pressure, and the reaction of internal jets have a larger influence.

14. KEY WORDS	LINK A		LINK B		LINK C	
	ROLE	WT	ROLE	WT	ROLE	WT
Recoil Mechanism						
Shock Absorber						
System Analysis						
Compressible Liquid						